ABIOTIC STRESS IMPACTS ON MACROPHOMINA ROOT ROT AND NANO-ENCAPSULATED CITRUS OILS TO CONTROL FRUIT AND FOLIAR PATHOGENS OF STRAWBERRY

A Thesis

presented to

the Faculty of California Polytechnic State University,

San Luis Obispo

In Partial Fulfillment

of the Requirements for the Degree

Master of Science in Agriculture, Specialization in Plant Protection Science

by

Marina Jade Gutierrez

December 2025

COMMITTEE MEMBERSHIP

TITLE: Abiotic Stress Impacts on Macrophomina Root Rot and Nano-Encapsulated Citrus Oils to Control Fruit and Foliar Pathogens of Strawberry

AUTHOR: Marina Jade Gutierrez

DATE SUBMITTED: December 2025

COMMITTEE CHAIR: Shashika S. Hewavitharana, Ph.D.
Associate Professor of Plant Sciences
Cal Poly, San Luis Obispo

COMMITTEE MEMBER: Gerald J. Holmes, Ph.D.
Director
Cal Poly Strawberry Center

COMMITTEE MEMBER: Andre S. Biscaro, M.S.
Irrigation and Water Resources Advisor
UC Cooperative Extension, Ventura

ABSTRACT

Abiotic Stress Impacts on Macrophomina Root Rot and Nano-Encapsulated Citrus Oils to Control Fruit and Foliar Pathogens of Strawberry

Marina Jade Gutierrez

Disease remains one of the major constraints to the productivity and economic success of the California strawberry industry. The most important soilborne pathogen is *Macrophomina phaseolina*, causing Macrophomina root rot (MRR). The most economically significant airborne pathogens include *Botrytis cinerea*, causing Botrytis fruit rot (BFR), and *Podosphaera aphanis*, causing powdery mildew (PM).

Disease severity of MRR is highly dependent on environmental factors. Therefore, understanding which abiotic stressors contribute most to disease development is crucial for effective management. A two-year field experiment at Cal Poly, SLO (2024 and 2025) evaluated the effects of drought stress, two elevated chloride stresses, and high EC_W stress on MRR development in two cultivars, Fronteras and Sweet Ann, that were artificially inoculated with *M. phaseolina.* Across both years, there was no significant treatment × cultivar interaction on final plant mortality ($P = 0.557$ and $P = 0.391$ for 2024 and 2025, respectively). In 2024 and 2025, treatment had a significant effect on final mortality ($P = 0.008$ and $P = 0.024$, respectively). Final mortality, averaged across both cultivars, was significantly higher in the drought stress treatment in 2024 (60.9%) and the high EC_W treatment in 2025 (47.3%), when compared to the standard treatment (37.2 and 19.9% in 2024 and 2025, respectively). Cultivar also had a significant effect on final plant mortality in both years ($P < 0.0001$ and $P < 0.0001$, respectively). ‘Sweet Ann’ consistently had higher final plant mortalities when compared to ‘Fronteras’ across both years. These results highlight the importance of utilizing cultural management tools, including maintaining optimal soil moisture using soil tensiometers, avoiding the use of

poor-quality irrigation water when possible, and planting disease resistant cultivars, to minimize disease severity.

Citrus essential oils have potential as biological controls that could limit crop losses due to foliar pathogens, reduce the use of synthetic fungicides, and slow resistance to major fungicide classes. However, low solubility and high volatility present barriers to practicality. Nano-encapsulation of essential oils offers a solution by improving dispersibility and retention of volatile bioactive compounds. Using commercially available citrus oil products that were nano-encapsulated (NE), preliminary trials were conducted to evaluate their efficacy against *B. cinerea* and *P. aphanis* across *in vitro*, *in planta*, greenhouse, and field settings at Cal Poly SLO. Treatments were pure citrus oils with the addition of an emulsifier, NE citrus oils containing 10% active ingredient (ai), and commonly used organic and conventional fungicides. Efficacy results were inconsistent across experiments. For the BFR experiments, NE citrus oils applied at 3 and 4% ai (v/v) significantly inhibited *B. cinerea* in detached fruit assays, when compared to the non-treated control (3%: $P = 0.045$; 4%: $P < 0.0001$). However, no significant inhibition was observed *in vitro* or in the postharvest evaluations of the field experiment, which may be due to product degradation over time. In the detached leaflet assay for PM, treatment had a significant effect on disease incidence ($P = 0.0178$) and observed phytotoxicity ($P < 0.0001$), but not disease severity ($P = 0.0552$). These results reveal limitations to the practicality of using NE citrus oils in commercial settings, including concerns of phytotoxicity and reduced product stability over time. Future work will evaluate the efficacy of NE citrus oils produced from Cal Poly harvested citrus against BFR and PM.

Keywords: Charcoal rot, Botrytis fruit rot, powdery mildew.

ACKNOWLEDGMENTS

Thank you to the USDA (Specialty Crop Research Initiative Project 2022-51181-38328) and the CDFA (Specialty Crop Block Grant 23-0001-031-SF) for funding these projects and making this work possible. I am grateful to the collaborators of the Macrophomina project, Dr. Peter Henry and Dr. Oleg Daugovish, and to our partners on the citrus oil project, Dr. Lauren Garner and the food technologists at Virginia Tech: Dr. Yiming Feng, Lihong Yang, and Sean Horner, and UC Riverside: Dr. Juhong Chen and Jason Zhai. The support of the Cal Poly Strawberry Center staff was instrumental to the success of both projects. Thank you to Vivian Longacre, Samantha Simard, Alexa Richardson, Kyle Blauer, Joseph Ramirez, Alison Stevens, and Colette Smith for all of their assistance. I would also like to thank fellow Strawberry Center graduate students Cooper Calvin, Maria Alvarez, Gabriela Torres, and Elias Barriga for their friendship and support, as well as undergraduate students: Emiliano Gomez, Stephen Pryor, Sydney Roncal, Marin Vargas, Kaela Higgins, Sophie Jerkovich, Shaelyn Spencer, Olivia Bruns, Cade Hibino, Derek Puckett, Jorge Rodriguez, and Aidan Inoue. I am grateful for my family, Jessie, Raul, and Alise, and to my partner Kaylie Di Paola, for their unwavering support and encouragement. Thank you to Andre Biscaro for serving on my graduate committee and for his guidance and collaboration on the Macrophomina project. Finally, thank you to Dr. Shashika Hewavitharana and Dr. Gerald Holmes for their continued mentorship and support. I am deeply grateful to have had the opportunity to work with both of them, and for the numerous opportunities they have opened for me.

TABLE OF CONTENTS

Page

LIST OF TABLES

LIST OF FIGURES

Chapter 1
LITERATURE REVIEW

1.1 Introduction

This literature review provides an overview of the California strawberry industry and current challenges with regard to disease prevalence and management practices. This thesis was focused on three major strawberry diseases: Macrophomina root rot caused by *Macrophomina phaseolina*, Botrytis fruit rot caused by *Botrytis cinerea*, and powdery mildew caused by *Podosphaera aphanis.* Current management practices were reviewed, with an emphasis on current trends in fungicide resistance, limitations of control methods, and the exploration of more sustainable alternatives to chemical controls, such as the implementation of cultural and biological controls.

1.2 The strawberry

The cultivated strawberry (*Fragaria* × *ananassa* Duch.) is an herbaceous perennial plant, belonging to the family *Rosaceae*. It is the most widely cultivated and economically significant species within the *Fragaria* genus (Davis et al. 2007). The cultivated strawberry originated from a hybridization between two octoploid species native to North and South America: *F. virginiana* and *F. chiloensis*, respectively (Darrow 1966). In the mid-1800s, the first formal breeding programs for cultivated strawberries were established in public institutions across England and America and during the twentieth century, private companies began to develop their own breeding programs (Davis et al. 2007). Early breeding efforts primarily focused on improving plant productivity and as global production and demand expanded, breeding objectives diversified to focus on improvements

in fruit quality, such as fruit appearance, size, color, flavor, shelf life, and resistance to important diseases (Darrow 1966).

Vegetatively propagated transplants, produced via runners (stolons), are used to establish clonal daughter plants in commercial fruit-producing fields. The vast majority of these transplants are produced by the California nursery industry at low (near sea level) and high elevation (1295 m) nurseries (Holmes 2024). Plants produced at low elevation nurseries are used for summer planting in California, which occurs between late May through early June, and for further plant production at high elevation nurseries (Holmes 2024). High elevation nurseries represent a majority of transplant production, as the environmental conditions allow for the proper conditioning of plants through sufficient chilling hours (Holmes 2024).

1.3 California strawberry industry

In 2023, the United States produced 1,250,100 tonnes of strawberries, ranking as the second largest strawberry producer worldwide after China (FAO 2023). In the US, the state of California is the leading producer of strawberries, producing approximately 90%, followed by Florida (CSC 2024a). In 2024, strawberries were ranked the fourth highest value crop in California, valued at $3.46 billion (CDFA 2024). The vast majority of strawberries produced in California are grown in one of the three major growing districts along the coast: Watsonville-Salinas, Santa Maria, and Ventura-Oxnard.

Strawberries are predominantly grown as an annual crop due to declines in yield and increases in pest pressures associated with second year production

(Strand 2008). A major threat to the industry's success are plant pests and diseases that significantly reduce crop productivity, decrease yield, and compromise fruit quality. Diseases can be categorized by their method of dissemination. Airborne pathogens affect foliage and fruit, and soilborne pathogens infect crown and root tissue, which in turn affect the entire plant. The most economically significant soilborne pathogen is *Macrophomina phaseolina*, while among the airborne pathogens, *Botrytis cinerea* and *Podosphaera aphanis*, are especially significant (Holmes 2024).

1.4 Abiotic stressors effect on plant physiology

Heat, drought, and elevated salinity are the most common environmental stressors which limit plant productivity by disrupting fundamental physiological and cellular processes (Zhang et al. 2022). When plants encounter these stressors, they exhibit two categories of responses: non-adaptive and adaptive (Zhang et al. 2022). Non-adaptive plant responses are reflections of damage caused by abiotic stressors such as physiological damage or disruptions to necessary cell functions. These non-adaptive responses to stress can be detrimental to the plant's survival under adverse conditions and often translate into visible injury. In contrast, adaptive plant responses allow plants to better cope under stress, improving overall stress resistance. This response may involve repairing stress-induced damage and the adjustment of growth patterns to optimize resource acquisition. Understanding the balance between these response types is crucial to understanding how crops will perform under changing environmental conditions.

1.4.1 Drought

Strawberry plants have a large demand for water because of their shallow root systems, large leaf area, and fruit containing high water content (Klamkowski and Treder 2006). As a result, they are particularly vulnerable to drought stress. When plants are exposed to drought conditions, there is a significant decrease in leaf water potential, leading to osmotic stress (Seleiman et al. 2021). In an effort to conserve water under these conditions, plants respond by closing their stomata, leading to decreased transpiration rates and reduced photosynthetic activity (Klamkowski and Treder 2006). To cope with drought conditions, morphological changes may be observed including the expansion of the root system such as increased root size, length, and density (Seleiman et al. 2021). Symptoms of drought stress appear as the increased rate of leaf senescence and drooping, leaf rolling, brittleness, and wilting (Seleiman et al. 2021).

1.4.2 Salinity

The strawberry is recognized as a crop that is very sensitive to salinity, with an electrical conductivity tolerance threshold of 1 dS/m (Maas and Hoffman 1977). When plants are exposed to elevated salinity, salts are transported into roots, which initially causes a reduction in leaf water potential, reducing leaf turgor and creating osmotic stress (Arif et al. 2020). With continued exposure, the concentration of toxic ions (Na^+ and Cl^-) continues to build in the cell cytoplasm, causing ionic stress that leads to the reduction in mineral uptake and the disintegration of cellular membranes (Arif et al. 2020). This significantly inhibits photosynthetic pathways such as chloroplasts and photosystem II, hampering

plant productivity. Plants respond to salinity stress by compartmentalizing excess ions and reducing transpiration rates (Turhan and Eriş 2007). As a result, symptoms of salinity damage on strawberry appear as chlorosis and marginal necrosis of the foliage (Al-Shorafa et al. 2014; Turhan and Eriş 2007).

1.5 Macrophomina root rot

Macrophomina root rot, also referred to as crown rot or charcoal rot, is caused by the soilborne pathogen *Macrophomina phaseolina*. This pathogen was first reported in California strawberry production in 2006, coinciding with the phaseout of the soil fumigant methyl bromide in fruit production systems (Koike 2008). By 2014, *M. phaseolina* had emerged as a prevalent and economically significant pathogen, with confirmed presence in all major growing districts throughout California (Koike et al. 2016). This pathogen is a necrotroph that utilizes cell wall degrading enzymes and toxins to populate root and stem tissues, attacking the plants vascular system. For this reason, symptoms first appear as the wilting of foliage and as the disease progresses, the infected plant will eventually collapse and die (Fig. 1.1). Disease development is favored by high air and soil temperatures between 28-35°C and soil with low moisture content (Wang et al. 2024; Zveibil et al. 2012).

1.5.1 Taxonomy and morphology

Macrophomina phaseolina (Tassi) Goid. belongs to the family *Botryosphaeriaceae* in the phylum Ascomycota. It can infect a wide range of plant hosts, with the current literature identifying at least 97 susceptible host species (Pennerman et al. 2024). *M. phaseolina* can produce dark, ostiolate

pycnidia and short, hyaline conidiophores that bear hyaline, ellipsoid conidia. However, these structures are rarely observed in natural settings (Kaur et al. 2012). Microsclerotia, which are smooth, black hardened masses of mycelia, serve as the primary source of inoculum as well as the pathogen's survival structure. Microsclerotia are produced in host tissues and can persist in the soil and plant residues for up to 15 years (Singh et al. 2023).

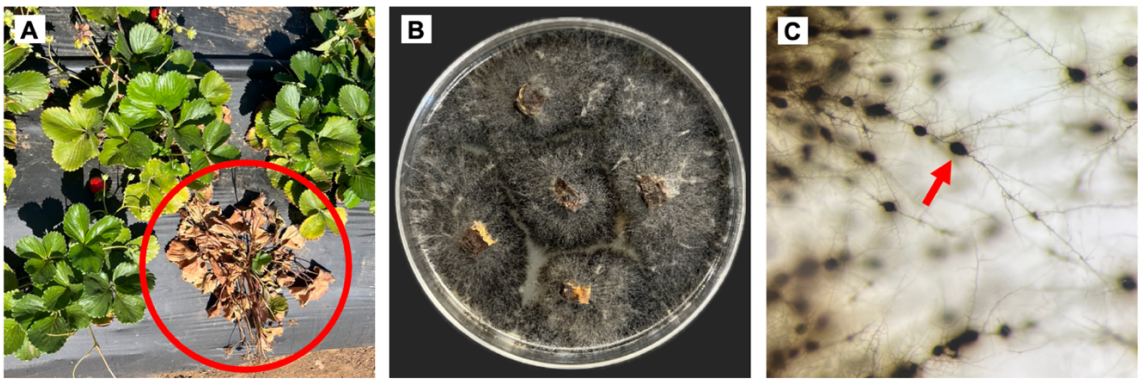

Figure 1.1. (A) Strawberry plant showing symptomatic collapse and death by *Macrophomina phaseolina*. (B) Infected crown tissue plated on half-strength acidified potato dextrose agar. (C) Microsclerotia of *M. phaseolina*.

1.5.2 Abiotic stressors

The severity of Macrophomina root rot is highly dependent on environmental factors, specifically exposure to abiotic stressors such as heat, elevated salinity, and drought. In several host crops, including chickpea and soybean, elevated air and soil temperatures have been associated with increased disease severity caused by *M. phaseolina* (Sharath Chandran et al. 2021; Teja et al. 2020). In strawberry, higher soil temperatures during plant establishment and air temperatures during the mid-season similarly exacerbate disease severity (Wang et al. 2024). Exposure of crops to elevated salinities has

been shown to increase disease severity of Macrophomina root rot in common bean and sorghum (Goudarzi et al. 2011; You et al. 2019). Further, an *in vitro* experiment demonstrated that the growth rate of *M. phaseolina* isolated on potato dextrose agar (PDA) plates increased when the medium was amended with salts (40 mM NaCl + 1 mM $CaSO_4$) (You et al. 2019). Low soil moisture levels significantly increase mortality of strawberry caused by *M. phaseolina* (Pedroncelli et al. 2025), while high soil moisture is associated with declines in viable *M. phaseolina* microsclerotia populations (Dhingra and Sinclair 1974). Collectively, these findings demonstrate that disease symptoms and plant mortality due to Macrophomina root rot are most severe when plants are under stress, which is why the pathogen is often described as an opportunistic parasite. This also indicates that disease severity can be mitigated by alleviating environmental stressors through the implementation of cultural management practices.

1.5.3 Disease management

Preplant fumigation remains the most effective and reliable form of control for managing *M. phaseolina* and can be further improved with the integration of cultural control practices (Holmes 2024). Cultural management strategies include crop rotation, planting disease-resistant cultivars, sanitation, and practices that minimize plant stress. For fields infested with *M. phaseolina*, the rotation of crops with non-susceptible hosts reduces the accumulation of colony forming units (CFU) within the soil that would otherwise increase with continuous strawberry production, while also promoting soil health and structure (Khalili et al. 2026).

Major strides in the breeding of disease-resistant strawberry cultivars have recently been made by phenotypic screening under heat and drought stress allowing for the identification of favorable alleles which can then be stacked to achieve quantitative resistance to *M. phaseolina* (Knapp et al. 2024). Although there are no completely resistant cultivars, Osceola has been identified as a highly resistant cultivar, while Monterey and Fronteras are considered moderately susceptible cultivars (Wang et al. 2024). Sanitation plays an essential role in limiting the spread of the pathogen by preventing the movement of infested soil. This involves disinfecting tools and equipment and removing infected crop residue at the end of the growing season to reduce the amount of CFU in the soil (Baggio et al. 2021b). Strategies for minimizing plant stress include maintaining optimal soil moisture levels and utilizing high quality irrigation water. However, not all growers in California have access to high quality irrigation water, highlighting the need for further research to investigate how elevated salinity impacts disease development of *M. phaseolina*.

The most commonly utilized preplant chemical fumigants are chloropicrin or chloropicrin mixed with 1,3-dichloropropene (Holmes et al. 2020). When distributed uniformly, soil fumigation significantly reduces the amount of *M. phaseolina* inoculum present in infested soils (Baggio et al. 2021b). Although there are conventional and organic products registered for use as pre-plant dips and soil drenches applied through drip irrigation systems, none have demonstrated consistent or significant efficacy and therefore have not been

widely adopted by growers in California (Blauer and Holmes 2019; Holmes et al. 2020).

1.6 Botrytis fruit rot

Botrytis fruit rot, the disease caused by *Botrytis cinerea*, is considered one of the most destructive diseases of strawberries worldwide (Romanazzi et al. 2022). *B. cinerea* is a necrotrophic fungus, meaning it secretes cell wall-degrading enzymes and toxins to first kill host cells and then colonizes and derives nutrients from the necrotic tissue. Symptoms of Botrytis fruit rot first appear as small brown lesions that continue to expand and become covered with gray fungal growth (Fig. 1.2). Disease development is favored by moderate to high humidities, leaf wetness durations of more than four hours, and temperatures between 15 and 25 °C (Jarvis 1962). The minimum temperature for growth is 0°C, indicating that *B. cinerea* is capable of developing during cold storage of produce (Romanazzi and Feliziani 2014). Control of this pathogen remains a challenge as it can cause severe losses at all stages of production. Strawberry fruit are susceptible to infection by *B. cinerea* in the field before harvest and during postharvest activities such as shipment and final sale (Romanazzi and Feliziani 2014). Another major challenge associated with *B. cinerea* is its classification as an organism that has a high risk of developing resistance to major classes of fungicides (Hahn 2014).

1.6.1 Taxonomy and morphology

Botrytis cinerea belongs to the family *Sclerotiniaceae* in the phylum Ascomycota. *Botrytis cinerea* is the asexual stage (anamorph) and *Botryotinia fuckeliana* is the teleomorph (Ellis and Waller 1974). It can infect a wide range of

plant hosts, with the current literature identifying more than 200 susceptible crop species (Williamson et al. 2007). *B. cinerea* produces long, branching conidiophores that bear gray, hyaline ellipsoidal conidia (Fig. 1.2). Mycelial branches fuse together to form sclerotia, the pathogen's survival structures, which provide protection from desiccation and UV radiation (Williamson et al. 2007).

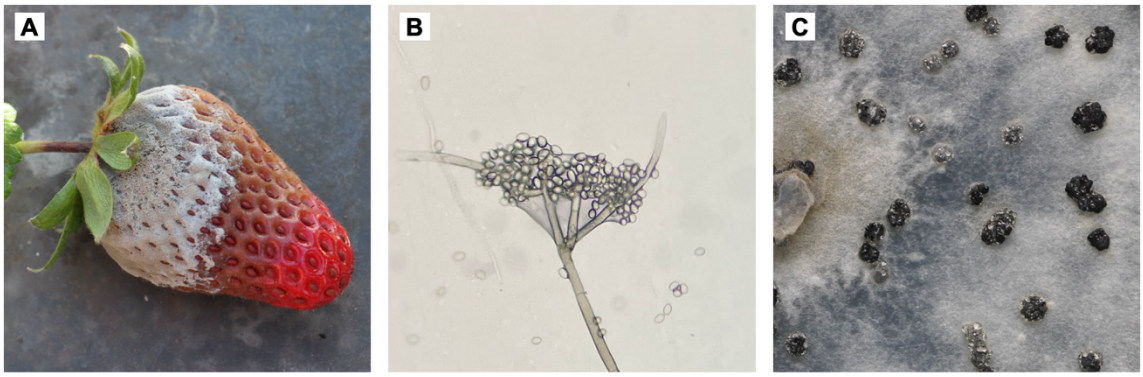

Figure 1.2. (A) *Botrytis cinerea* infection on strawberry fruit (photo by G. J. Holmes). (B) Branching conidiophore bearing conidia and (C) sclerotium of *B. cinerea* (photo by G. J. Holmes).

1.6.2 Disease management

Cultural control strategies can be implemented to control *B. cinerea,* but the use of chemical controls remains the most efficient and cost-effective method (Mertely et al. 2000). Cultural practices involve sanitation and modifications to plant microclimates to minimize conditions conducive to pathogen growth (Mertely et al. 2000). Sanitation involves the removal of infected plant material and debris to reduce the amount of inoculum present. Microclimate modifications focus on reducing relative humidity around individual plants. Production in large plastic tunnels significantly reduces incidence of Botrytis fruit rot by decreasing

periods of leaf wetness as well as light intensity (Xiao et al. 2001). However, these environmental modifications may exacerbate other disease pressures including powdery mildew (Xiao et al. 2001). The adoption of wider plant spacing significantly reduces the incidence of *B. cinerea* throughout the growing season, however there is a trade-off as marketable yields are also reduced by wider spacing (Legard et al. 2000). The utilization of drip irrigation instead of overhead irrigation and the trimming of necrotic and senescent leaves throughout the growing season are other cultural methods utilized by growers to reduce relative humidity (Mertely et al. 2000). Host resistance is not a viable option, as all current commercial cultivars are susceptible to infection by *B. cinerea*, despite some variation in the degree of susceptibility (Legard et al. 2000).

To achieve efficient control of *B. cinerea* using chemical controls, the timing of fungicide sprays is critical. Strawberry flowers are more susceptible to *B. cinerea* than green developing fruit, thus preventative fungicide sprays during peak bloom periods will provide the most effective control while also minimizing fungicide use (Mertely et al. 2002). Disease forecast systems, such as the Strawberry Advisory System (StAS), have demonstrated strong efficacy in reducing losses due to *B. cinerea* while simultaneously lowering the number of total fungicide applications (Cordova et al. 2017). The use of predictive models has become widely adopted by strawberry growers in Florida and have significant potential for adoption in California (Cordova et al. 2017; Ramirez 2024).

Products approved for organic production are limited, and while some provide partial control of *B. cinerea*, their overall effectiveness remains low (Adaskaveg et al. 2025). Organic products include inorganic compounds and biological agents such as essential oils and microorganisms (Dwivedi et al. 2025).

1.7 Powdery mildew

Strawberry powdery mildew is a disease caused by *Podosphaera aphanis* Wallr. (formerly *Sphaerotheca macularis*). This pathogen is an obligate biotroph, meaning that living host tissue is required for the pathogen to complete its lifecycle. Symptoms of the disease appear as curling of the leaf margins and purple-red blotches on the lower leaf surface (UC IPM 2018). Infection by *P. aphanis* will generally establish first on the underside of leaves, and fungal colonies will appear as powdery white patches of mycelial growth observed on leaves, petioles, and fruit (UC IPM 2018). Disease development is favored by a relative humidity over 75% and temperatures between 15 and 26 °C (Amsalem et al. 2006). According to the Fungicide Resistance Action Committee (FRAC 2019), *P. aphanis* is recognized as a ‘medium risk’ organism to develop resistance to fungicides.

1.7.1 Taxonomy and morphology

Podosphaera aphanis belongs to the family *Erysiphaceae* in the phylum Ascomycota. It has a restricted host range, as the only reported host of *P. aphanis* is strawberry. *P. aphanis* produces hyaline conidiophores that bear chains of hyaline, ellipsoidal conidia (Fig. 1.3). Chasmothecia bear sexual ascospores and serve as the pathogen’s overwintering structure. Warm climates

suppress the initiation of chasmothecia, which is likely why the incidence of this structure is reportedly rare in California strawberry-growing regions (Asalf et al. 2013). In the absence of chasmothecia, *P. aphanis* primarily overwinters as dormant mycelia on plant tissue.

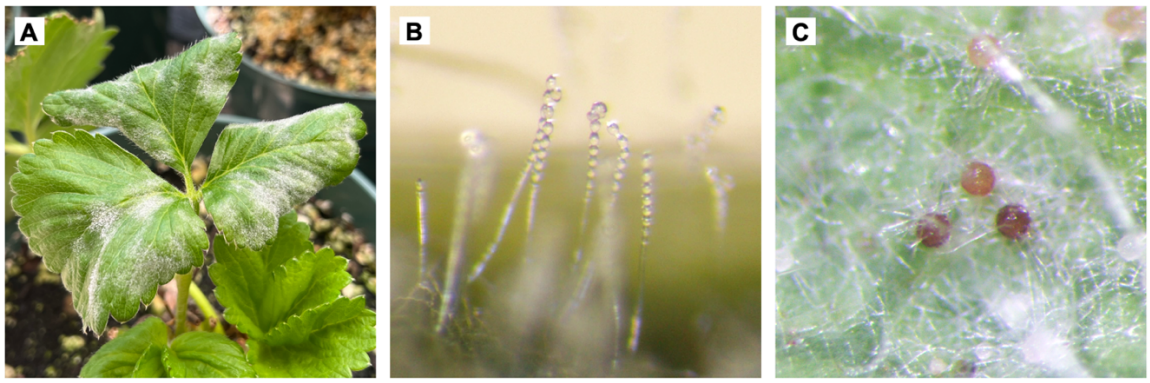

Figure 1.3. (A*) Podosphaera aphanis* infection on strawberry leaves. (B) Conidiophore bearing chains of conidia and (C) chasmothecia of *P. aphanis*.

1.7.2 Disease management

The use of cultural and chemical controls are the most effective methods of controlling powdery mildew. Cultural controls function primarily as preventative measures and include the use of disease-resistant strawberry cultivars and modifications to the growing environment to suppress conditions favorable for disease development. Planting resistant cultivars is highly beneficial as it reduces reliance on chemical controls. However, resistant cultivars do not always achieve commercially acceptable fruit yield or quality standards (Menzel 2021). In California, there are currently no strawberry cultivars that are completely resistant to *P. aphanis*, but several have been identified as moderately resistant such as San Andreas and Sweet Ann (Palmer and Holmes 2022). Midday pulsed water misting through overhead irrigation can effectively remove mature conidia from

plant surfaces, reducing the amount of viable *P. aphanis* inoculum (Asalf et al. 2020). However, this practice can inadvertently create conditions conducive for *B. cinerea*. Strawberry grown in controlled environments, such as plastic tunnels or greenhouses, observe significantly higher severities of powdery mildew due to conditions of low light intensity and high relative humidity without free moisture (Xiao et al. 2001).

Ultraviolet (UV) irradiation can be utilized as a form of physical disease control. Applying low doses of UV irradiation followed by a four-hour dark period has been shown to significantly reduce powdery mildew incidence (Janisiewicz et al. 2016). Recent advancements in application technology, such as the development of a robotic UV-delivery apparatus, have made this form of control more practical for use in open-field production (Onofre et al. 2021a).

Chemical controls remain a central component of powdery mildew management, especially when integrated with cultural practices. A wider range of products approved for use in organic production are available for control of *P. aphanis*, several of which provide adequate levels of efficacy (Adaskaveg et al. 2025). Among these, sulfur remains the most commonly used product in both organic and conventional production systems (DPR 2023). When applied preventatively and at appropriate intervals, sulfur can significantly reduce foliar disease severity in open-field and tunnel production systems, providing levels of control comparable to conventional fungicides (Onofre et al. 2021b).

1.8 Fungicide resistance

The introduction of site-specific fungicides, which inhibit a critical biochemical function of fungi, was initially highly effective but their long-term efficacy is currently threatened by the rapid emergence of resistant pathogen populations (Hahn 2014). Fungicide resistant fungal populations develop as a result of the selection pressure that occurs each time a single-site fungicide is applied: the sensitive population is killed and the resistant mutants remain, allowing them to proliferate (Hobbelen et al. 2014). Resistant isolates of both *B. cinerea* and *P. aphanis* have been reported in all major strawberry growing regions in California (Cosseboom et al. 2019; Palmer and Holmes 2021). For *B. cinerea*, resistance has been documented in all major site-specific chemical classes (Cosseboom et al. 2019). Similarly, compromised efficacy has been documented for most fungicides that are currently used for control of *P. aphanis* (Palmer and Holmes 2021). Given these trends, resistance management has become a critical component of disease control programs. Strategies to prevent the accumulation of resistant populations include scouting, monitoring, and disease forecast systems such as the Strawberry Advisory System (StAS) to determine when the use of fungicides is necessary (Cordova et al. 2017), prioritizing the use of multisite over site-specific fungicides when possible, and the rotation of fungicides that target different essential biochemical pathways of pathogens (UC IPM 2025). There are currently no equivalent alternatives that can match the efficacy and reliability of chemical fungicides, underscoring the

necessity of exploring and developing biological controls as a potential alternative (Hahn 2014).

1.9 Essential oils as biological controls

Essential oils are naturally derived plant extracts with complex chemical compositions which exhibit broad antimicrobial activities (El Asbahani et al. 2015). Among these, the essential oil of citrus is of particular intrigue for use within agricultural settings. Citrus peel waste is generated in large quantities within major production regions such as California, making these oils abundant and inexpensive (Callaway et al. 2011). In postharvest settings, the application of citrus essential oils demonstrated effective control of fruit rot diseases. Shehata et al. (2020) reported that lemon, orange, and mandarin essential oils applied as postharvest treatments to strawberry effectively reduced the incidence of fruit rot and extended the shelf-life in cold storage. Furthermore, citrus oils are generally accepted as a safer alternative to synthetic chemical fungicides and are recognized as Generally Recognized as Safe (GRAS) by the US Food and Drug Administration (Callaway et al. 2011). These findings highlight the potential of utilizing citrus oils as biological control agents against strawberry pathogens.

1.9.1 Antifungal properties

The antifungal efficacy of essential oils is highly dependent on the chemical composition, persistence of active compounds over time, and the duration of exposure to the target pathogen (Khetabi et al. 2022). Essential oils extracted from citrus waste consists of major biologically active compounds including *d*-limonene (Shehata et al. 2020). *D*-limonene plays a central role in

fungal inhibition, with the primary mode of action involving the disruption of fungal cell membranes and cell wall integrity. Treatments of *d*-limonene to fungal pathogens have been shown to increase cell permeability, compromise structural stability, decrease resistance to heat, and ultimately lead to the leakage of intracellular material including proteins, lipids, and nucleic acids (Lin et al. 2024). However, as with many other essential oil compounds, the properties of *d*-limonene limit its practical applications (Lin et al. 2024).

1.9.2 Limitations

The hydrophobic and volatile nature of bioactive molecules in essential oil pose a challenge for their direct incorporation into agricultural production settings (Donsì and Ferrari 2016). After extraction from plant materials, essential oils are highly susceptible to degradation caused by environmental factors such as elevated temperatures, UV radiation, and exposure to oxygen (Turek and Stintzing 2013). Such degradation would progressively diminish a product's chemical stability and uniformity over time, ultimately comprising product efficacy during storage and application. Another major constraint to commercial use of essential oils is the occurrence of plant injuries from exposure to essential oils, known as phytotoxicity (Werrie et al. 2020). Although many essential oils exhibit potent antimicrobial activities, these same compounds can cause unintended phototoxic injuries to plant tissues and considerable precautions must be taken to prevent this (Werrie et al. 2020). Symptoms of damage can range from leaf deformation, chlorotic or necrotic lesions on foliage, and scarring of fruit, all of which threaten crop yield and fruit marketability. Collectively, these constraints

underscore the importance of developing an effective delivery system that addresses the current limitations.

1.9.3 Nano-encapsulation

The encapsulation of essential oils in oil-in-water emulsions, or nano-emulsions, may provide a solution to the limitations associated with using pure essential oils as biological control agents (Ali et al. 2017). Nano-emulsions consist of very small oil droplets, typically ranging from 20 to 200 nm, that are dispersed in an aqueous solution and stabilized by the addition of an emulsifier (Donsí and Ferrari 2016). To achieve these small droplet sizes, physical dispersion methods such as ultrasonication and high-pressure homogenization are utilized to prepare nano-emulsions (Donsí and Ferrari 2016). This nano-encapsulation of essential oils can improve the solubility and stability of bioactive compounds against volatilization, while maximizing antimicrobial activity (Miastkowska et al. 2020). Foliar applications of nano-encapsulated celery seed oils have demonstrated better inhibition of *Podosphaera fusca*, the causal agent of cucumber powdery mildew, compared to the control achieved by pure oils under greenhouse conditions (Soleimani et al. 2024; Soleimani et al. 2023). However, phytotoxic symptoms were observed across both nano-encapsulated and pure oil products, suggesting that nano-emulsions may not fully mitigate plant safety concerns. Although there are some publications evaluating fungicidal efficacy of nano-emulsions within field or greenhouse settings, a large majority of published research remains limited to *in vitro* or postharvest assays. This necessitates a study to evaluate the efficacy of nano-encapsulated essential oils

across a broader range of contexts including *in vitro*, *in planta*, greenhouse, and field assays in order to gain a more comprehensive understanding on product efficacy, phytotoxicity potential, and practical feasibility in commercial production systems.

1.10 Conclusions

The prevalence of soilborne and airborne diseases pose a major threat to the success of the California strawberry industry, especially as regulations on pesticide and fumigant use continue to increase. The implementation and further development of cultural and biological controls are promising alternatives to reduce reliance on chemical fungicides. The first objective of this thesis is to evaluate the effect of abiotic stressors on disease development of Macrophomina root rot. The second objective is to evaluate the efficacy of using nano-encapsulated citrus oils to control strawberry pathogens causing Botrytis fruit rot and powdery mildew. Both objectives focus on building upon current management strategies through the exploration of sustainable approaches to disease management.

Chapter 2

EFFECT OF ABIOTIC STRESSES ON MACROPHOMINA ROOT ROT DEVELOPMENT IN CALIFORNIA STRAWBERRY

2.1 Introduction

California accounts for approximately 90% of strawberry production within the United States and in 2024, the industry was valued at $3.46 billion, solidifying strawberries as California's 4th highest grossing crop behind almonds, grapes, and lettuce (CDFA 2024). In recent years, soilborne pathogens have increasingly become a major threat to the industry's success.

In 2016, the soil fumigant methyl bromide was fully phased out for use in strawberry fruit production, though it remains an important management tool for strawberry nurseries to prevent the spread of disease and pests on planting stock (Holmes et al. 2020). This phase-out within fruit production consequently led to increased yield losses due to the emergence of soilborne pathogens, including *Macrophomina phaseolina*, the causal agent of Macrophomina root rot (Koike et al. 2013). Symptoms of the disease appear as plant stunting, wilting of foliage, drying and death of older leaves, and the eventual collapse and death of the entire plant (Koike 2008). Recently conducted surveys on disease incidence within California strawberry production reveal that *M. phaseolina* is prevalent within all three major strawberry-growing districts at the following rates: 29.7% in Watsonville-Salinas, 52.0% in Santa Maria, and 67.6% in Ventura (Simard 2024; Steele et al. 2024; Steele et al. 2023). This pathogen produces survival structures called microsclerotia, which have an excellent tolerance to a variety of

adverse environmental conditions (Dahikar and Nagarkar 2023) and can persist in host residues within soil for up to 15 years (Sarr et al. 2023), complicating management efforts. Moreover, *M. phaseolina* has wide host range of at least 97 plant host species (Pennerman et al. 2024).

Current management practices for conventional growers are heavily reliant on pre-plant fumigation. Chloropicrin applied on its own or in combination with 1,3-dichloropropene are the most widely used fumigants (Holmes et al. 2020), though these alternatives are not as efficacious as the former standard, methyl bromide (Duniway 2002). With increasing regulatory pressure on pesticide use in California, there is a growing need for sustainable, yet practical, disease management strategies that growers can readily use. Development of improved cultural control strategies such as crop rotation, planting disease resistant cultivars, improved sanitation, and managing plant stress, offer a promising solution (Singh et al. 2023).

Previous research has shown that host plant exposure to abiotic stressors can further exacerbate Macrophomina root rot progression, which is why the pathogen is often described as an opportunist. Drought, elevated soil salinity, and heat have been identified as major stressors that predispose plants to infection by *M. phaseolina* on crops such as sorghum, soybean, common bean, and chickpea (Chilakala et al. 2022; Goudarzi et al. 2011; Kendig et al. 2000; You et al. 2011). Although much of the existing research on abiotic stressors has focused on other crops, there have been few studies examining how they affect Macrophomina root rot development specific to strawberry production systems.

High soil temperatures and low soil moisture have been shown to significantly increase plant mortality caused by *M. phaseolina* (Pedroncelli et al. 2025; Wang et al. 2024). Strawberry plants grown under saline conditions exhibit significant reductions in vegetative growth and fruit yield (Al-Shorafa et al. 2014; Maas and Hoffman 1977), reinforcing its classification as a salt-sensitive crop. However, interactions between salinity stress and *M. phaseolina* within strawberry production have not been sufficiently studied. To our knowledge, the comparison of drought and elevated salinity stress on Macrophomina root rot development within field-grown strawberry has not been described. The objective of this study is to identify which stressors contribute most to Macrophomina root rot disease development in order to identify practical management strategies that growers can use to mitigate disease severity.

2.2 Materials and methods

2.2.1 Field site

This experiment was conducted at California Polytechnic University, San Luis Obispo, in field 35b (35.30569°N, 120.67357°W). The soil type of field 35b is classified as Salinas silty clay loam on a 0-2% slope, as stated on SoilWeb (California Soil Resource Lab, UC Davis/UC-ANR/USDA NRCS, https://casoilresource.lawr.ucdavis.edu/gmap/). This field has been repeatedly infested with *Macrophomina phaseolina* for eight consecutive years which has led to the buildup of high levels of *M. phaseolina* colony forming units (CFU). In 2023, a pour plate method adapted from Cloud and Rupe (1991) was used to quantify the inoculum level present in the soil and was determined to have an

average of 22 CFU/g (Steele 2023). During the 2024 experiment, *Fusarium oxysporum* f. sp. *fragariae* race 1 was identified in the field for the first time. In an attempt to eradicate this pathogen, the field was flat fumigated with Tri-Clor (99.0% chloropicrin; TriCal Inc., Hollister, CA) at a rate of 300 lb/A on 9 September 2024 before bedding up and planting for the 2025 experiment. Post-fumigation, the *M. phaseolina* inoculum level was reduced to 3 CFU/g.

2.2.2 Inoculum production and inoculation

The production of *M. phaseolina* inoculum was adapted from Mihail (1992). Autoclaved containers (Nalgene, Rochester, NY) were filled with aquatic sand substrate (Petco, San Diego, CA), cornmeal (Quaker, Chicago, IL), and deionized water in a ratio of 1:0.4:0.4. The mixture was autoclaved for 60 min, mixed, autoclaved for a second time after a 24 h interval, and mixed again. Once the mixture cooled to room temperature, it was infested with four to five 5 mm^2 agar plugs from one-week-old *M. phaseolina* cultures. Three *M. phaseolina* isolates were used for this experiment in 2024 (Mp 70, Mp 96, and Mp 102) and 2025 (Mp 92, Mp 96, and Mp 110). Infested containers were incubated at 32°C for seven days and shaken once per day by hand to ensure uniform colonization. Colonized cornmeal-sand mixtures were then air dried on metal trays for five days and stored at room temperature in the dark prior to use.

Bare-root strawberry transplants of cultivars Fronteras and Sweet Ann were planted on 1 November 2023 for the first year of the experiment and 31 October 2024 for the second year. These cultivars were chosen based on their susceptibility to infection by *M. phaseolina*. ‘Fronteras’ is moderately susceptible

to Macrophomina root rot and ‘Sweet Ann’ is highly susceptible (Wang et al. 2024). Strawberry transplants were allowed two weeks to establish and then artificially inoculated with 5 g of *M. phaseolina* cornmeal-sand inoculum (1163 and 1034 CFU/g, in 2024 and 2025, respectively) mixed into the soil around the exposed crown tissue of each plant.

2.2.3 Experimental design

The five treatments consisted of a control, a drought stress, two elevated chloride stresses, and a high electrical conductivity (EC_W) stress. The treatments were assigned to experimental units according to a split-plot randomized complete block design (RCBD), with the stress treatment as the whole plot and the cultivar as the subplot with four replicates. Subplots contained 44 plants of ‘Fronteras’ or ‘Sweet Ann,’ and were 4.3 m-long of a 1.1 m-wide industry standard raised bed with a 0.7 m buffer between each treatment.

For irrigation, high-flow drip tapes (Toro, Bloomington, MN) (2.73 liter/min at 8 psi, 20 cm spacing between emitters) were laid 2.5 cm below the soil surface of raised beds. In 2024, three drip tape lines were laid placing one line between two plant rows. In 2025, to increase irrigation uniformity, the number of drip tape lines was reduced to two, with one line placed between the outer and middle plant rows. Solar-powered soil tensiometers (Hortau, San Luis Obispo, CA) were installed at a 45° angle so that the ceramic tip was located beneath the plant root system (15 and 30 cm below the soil surface in 2024 and 15 cm below the soil surface in 2025). In 2024, four tensiometers were installed: two placed in a standard and two in a drought treatment plot, positioned in the outer and center

plant rows. In 2025, eight tensiometers were installed: two placed into each cultivar subplot within a standard and a drought treatment plot, positioned in the two center plant rows to avoid edge effects.

Tensiometers' readings were recorded every 15 minutes and read daily to determine the frequency of irrigation. The drought treatment only received irrigation once the average soil tension at 15 cm depth reached approximately 60 kPa whereas all other treatments received irrigation once soil tension reached 10 kPa. For the salinity stress treatments, concentrated salt solutions were mixed (Table 2.1) and stored within three plastic 208-liter drums (Fig. 2.1). The salts used were: $CaCl_2$ (OxyChem, Ludington, MI), $MgCl_2$ (Zechstein Minerals BV, Veendam, Netherlands), NaCl (Morton Salt, Chicago, IL), Na_2SO_4 (Searles Valley Minerals, Trona, CA), and $MgSO_4$ (Premier Magnesia, LLC, Waynesville, NC). Water-powered dilution pumps (Dosatron, Clearwater, FL) were placed above each drum of salt solution and used to incorporate the salt solutions into the irrigation water at a diluted rate. Salt solutions were mixed for one minute prior to each irrigation and applied with every irrigation event. Drought stress treatments required little to no irrigation during the early season (December to April), due to precipitation and cooler temperatures, and received irrigation about twice per week for the remainder of the experiment (May to August). All other treatments received irrigation about once per week during the early season and up to three times per week when temperatures peaked.

Treatments in 2024 began on 19 March and concluded on 6 August. Heavy rainfall received during December 2023 through March 2024 delayed the

initial onset of treatments within the first year of the experiment. In 2024, the drought stress treatments received 20 irrigation events totaling 9,351 liters, and the standard treatments received 38 irrigation events totaling 22,503 liters. Treatments in 2025 began on 17 January and concluded on 7 August 2025. In 2025, the drought stress treatments received 28 irrigation events totaling 26,611 liters, and the standard treatments received 47 irrigation events totaling 41,410 liters.

Water samples were collected from the end of each plot's drip tape on 11 June 2024 and 12 June 2025 and analyzed by commercial laboratories to determine $EC_{W,}$ chloride (Cl), and sodium adsorption ratio (Table 2.1). Soil samples were collected from 0-15 cm depth, taken before the start of the experiment (December) and at the end of the experiment (September 2024 and July 2025), to evaluate soil salinity levels (Table 2.2).

Table 2.1. Added salts, chloride amount, sodium absorption ratio (SAR), and electrical conductivity of irrigation water (EC_W) for all treatments within 2024 and 2025

		2024			2025		
Treatment	**Added salts**	**Chloride (meq/liter)**	**Sodium absorption ratio (SAR)**	**EC_W[a] (dS/m)**	**Chloride (meq/liter)**	**Sodium absorption ratio (SAR)**	**EC_W[b] (dS/m)**
Standard	No added salts	0.77	0.60	0.74	0.73	0.60	0.70
Drought	No added salts	0.77	0.60	0.74	0.73	0.60	0.70
Chloride	$CaCl_2$, $MgCl_2$, NaCl	5.21	0.80	1.26	6.20	0.90	1.36
Chloride × 2	$CaCl_2$, $MgCl_2$, NaCl	7.92	1.00	1.52	13.00	1.10	2.09
High EC_W	$MgSO_4$, Na_2SO_4, $MgCl_2$, NaCl	2.46	2.10	1.98	3.70	1.80	2.19

[a] Analysis conducted at UC Davis Analytical Laboratory, Davis, CA.
[b] Analysis conducted at Fruit Growers Laboratory Inc., Santa Paula, CA.

Table 2.2. Soil salinity levels before the start and at the end of the 2024 and 2025 experiments

	2024				2025			
	December [a]		September [a]		December [a]		July [b]	
Treatment	**EC_e (dS/m)**	**SAR**	**EC_e (dS/m)**	**SAR**	**EC_e (dS/m)**	**SAR**	**EC_e (dS/m)**	**SAR**
Standard							0.66	1.06
Chloride							1.55	1.33
Chloride × 2	1.86	0.80	1.91	0.70	1.39	0.80	1.94	1.68
High EC_W							2.80	2.71
Drought							0.66	1.06

[a] Analysis conducted at A&L Western Laboratories, Inc., Modesto, CA.
[b] Analysis conducted at Fruit Growers Laboratory, Inc., Santa Paula, CA.

From the irrigation setup (Fig. 2.1), 2.5 cm tubing delivered the treatment directly to each experimental plot, into drip irrigation tapes. Flowmeters were installed at the transition between PVC pipe to 2.5 cm tubing in order to calibrate all dilution pumps to a 1% solution output. To calibrate, 10-liters of each concentrated salt solution was measured into three 19-liter buckets. Tubing responsible for drawing up salt solutions into the dilution pump mixing chamber was placed into the 19-liter buckets and irrigation was run for one hour. Once irrigation stopped, the remaining solution within each 19-liter bucket was remeasured in order to determine the amount of solution that was injected into the field. Those values were then divided by the total liters of irrigation applied to the field, determined by the flowmeters, to find the output percentage of each concentrated solution.

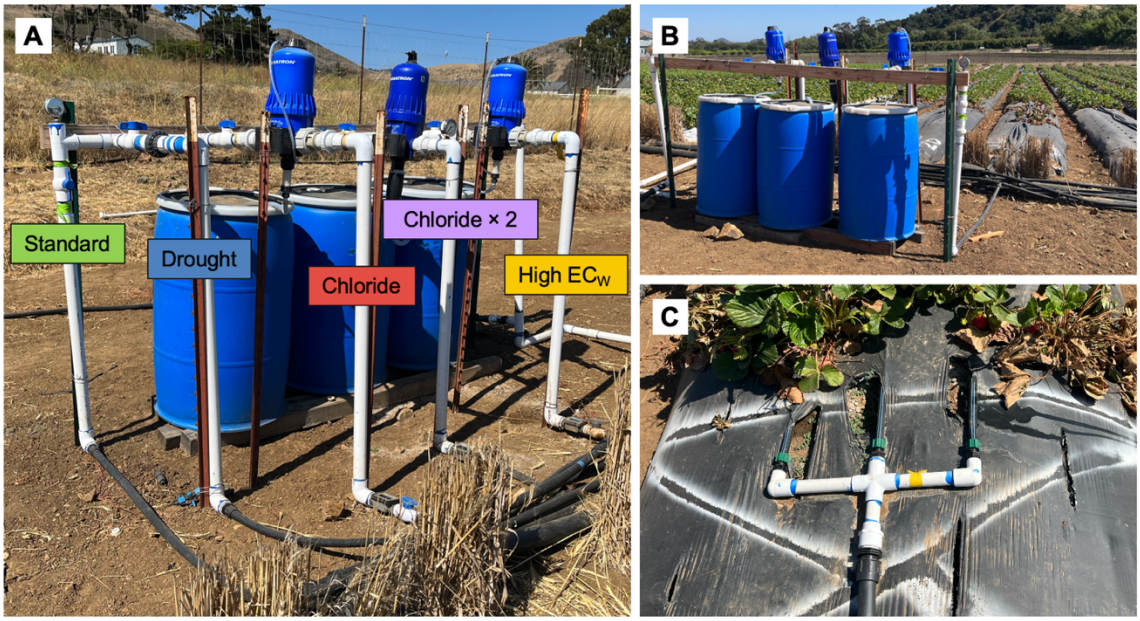

Figure 2.1. (A) Irrigation setup labeled by treatment type. (B) Setup located at the end of the beds near the irrigation source. (C) Individual irrigation tubing leading out from setup pictured in A and B, to each treatment plot.

2.2.4 Plant mortality

To determine plant mortality rates, the experiment was visually assessed weekly starting one month after the first treatments were applied and continued until the experiment concluded. Plants with at least 75% necrotic foliage were recorded as 'dead' and removed. Partially necrotic plant tissue was taken from each dead plant and plated onto selective media in order to confirm the presence of *M. phaseolina* and to screen for the presence of additional pathogens. The number of plants per plot was adjusted to exclude any plants that died due to pathogens other than *M. phaseolina*. Crown tissue was cut into 1 cm^3 pieces and petioles and secondary or tertiary roots were cut to 1 cm segments. Plant tissue was plated onto several selective media to screen for pathogen presence: Sorensen's NP-10 medium (Kabir et al. 2004) for *Verticillium dahliae* and *M. phaseolina*, PARP medium (pimaricin + ampicillin + rifampicin + pentachloronitrobenzene; Erwin and Ribeiro, 1996) for *Phytophthora* and *Pythium* spp., and half-strength acidified potato dextrose agar (APDA) as a general-purpose fungal medium. Plant tissue plating was conducted as follows: three petioles and two crown pieces on NP-10, three roots and two crown pieces on PARP, and four crown pieces on APDA. This continued until *M. phaseolina* was isolated from 90% of the collected samples and the process was simplified by plating only crown tissue onto APDA. After *M. phaseolina* was isolated from at least 95% of the samples, all plant mortalities were assumed to be caused by *M. phaseolina*. *Fusarium oxysporum* f. sp. *fragariae* race 1 was identified as the

cause of death for 2.5% of the plants plated in 2024 and less than 1% of plants plated in 2025.

Disease incidence was calculated as the number of dead plants due to *M. phaseolina* compared to the total number of plants per plot. Mortality assessment data was used to calculate area under the disease progress curve (AUDPC), using the following formula (Jeger and Viljanen-Rollinson 2001):

$$\text{AUDPC} = \sum_{i=1}^{N_{i-1}} \frac{(y_i + y_{i+1})}{2} \times (t_{i+1} - t_i)$$

N represents the total number of observations, y_i is the percent mortality for the observation number *i*, and t_i represents the number of days from the planting date.

2.2.5 Fruit yield

In 2024, fruit yield data was collected weekly, for three consecutive weeks, during peak fruit production (May) and during the late season (July). These production intervals were determined by reviewing the annual fruit volume trends for day neutral strawberries grown in the Santa Maria district (CSC, 2024b). In 2025, fruit yield data was collected throughout the entire season, once per week during the early-season (March to April) and at three-day intervals during the peak- and late-season (May to July). Ripe fruit were harvested and weighed. Each fruit was then visually inspected and classified as either marketable or unmarketable. Fruit considered unmarketable included strawberries that were too small (< 4 cm in length), misshapen, or showing signs of rot or insect damage (Fig. 2.2). Unmarketable fruit was removed, and the remaining fruit was weighed again to determine marketable fruit weight.

In 2024, the fertilizer calcium nitrate (17-0-0) was applied at a rate of 3 kg N/ha/week during the early-season and 6 kg N/ha/week during the peak- and late-season. In 2025, nitrogen fertilization was increased to better reflect commercial production practices: ammonium nitrate (20-0-0) fertilizer was applied at a rate of 5 kg N/ha/week during the early-season and 10.6 kg N/ha/week during the peak- and late-season.

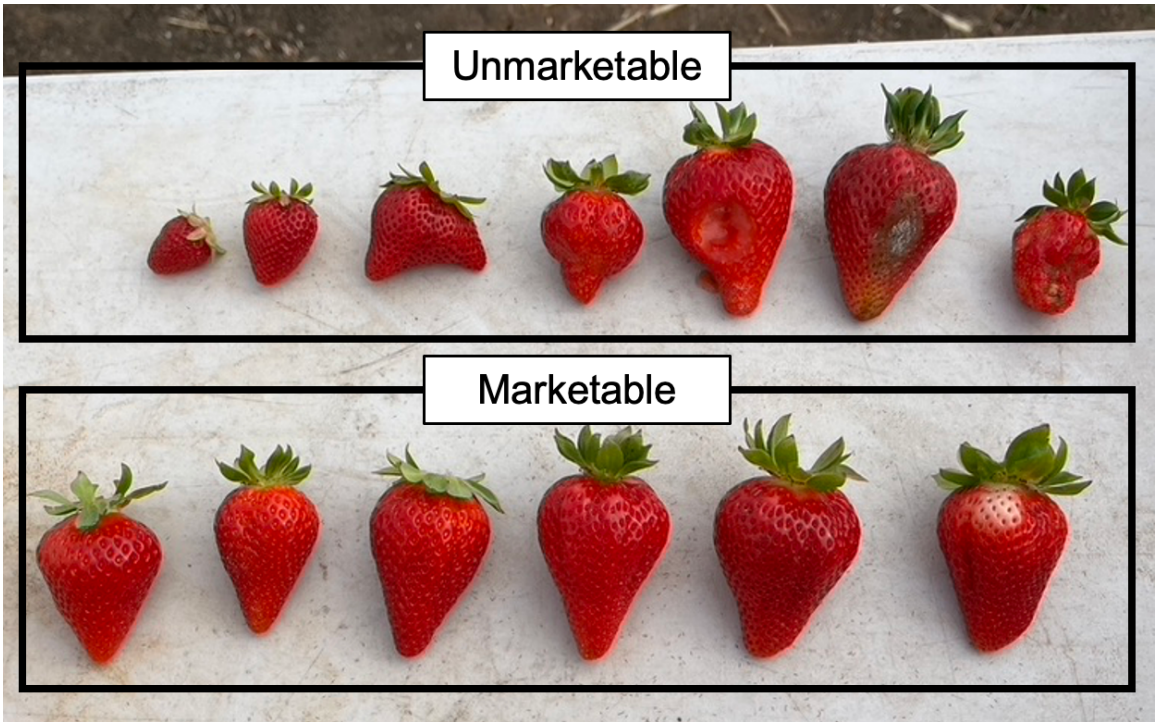

Figure 2.2. Examples of fruit considered unmarketable (top row) and marketable (bottom row).

2.2.6 Salt stress symptom assessment

Weekly visual assessments of salt-related injuries present on plant foliage began on 21 June 2024 and 3 July 2025. The visual assessment rating scales were adapted from Ledesma et al. (2016). Each subplot received two scores between 0-100; one score represented leaf margin necrosis: 0 = no necrosis, 100

= 100% of foliage is necrotic, and the other score represented chlorosis: 0 = no yellowing, 100 = 100% of foliage is yellow (Fig. 2.3). Severity scores indicated the mean score among all plants within one subplot. Aerial images of subplots, taken by a AgEagle RedEdge MX Dual Camera multispectral drone (aerialPLOT, Troy, OH), were also utilized to assess salinity symptoms. Aerial images were taken every three weeks during the early season (October to April) and every two weeks during the peak- and late-season (May to August). To determine necrosis levels, leaf area index (LAI) quantified the area of visible green leaf tissue within each subplot. To determine chlorosis levels, normalized difference red-edge index (NDRE) measured the chlorophyll levels within each subplot. Aerial imaging data were then compared to data collected by visual assessment using a correlation matrix.

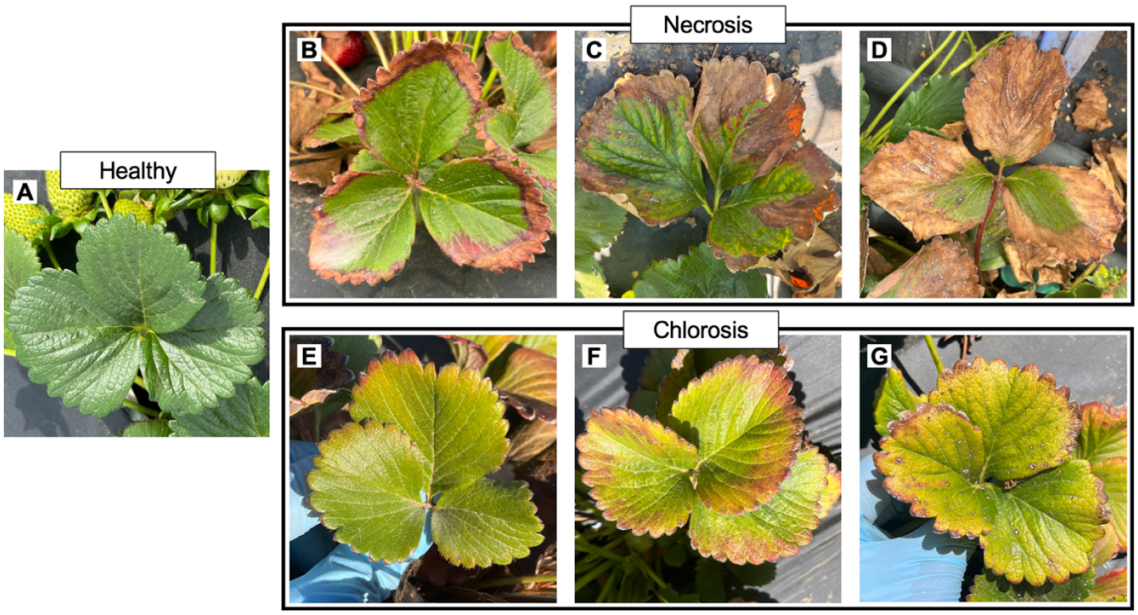

Figure 2.3. Example of salinity symptom ratings. (A) 0 = healthy leaf tissue; Leaf margin necrosis of: (B) 25% of leaf tissue, (C) 50% of leaf tissue, (D) 75% of leaf tissue; Chlorosis of: (E) 25% of leaf tissue, (F) 50% of leaf tissue, (G) 75% of leaf tissue.

2.2.7 Weather data collection

Annual rainfall, air temperature, and soil temperature data were obtained from the California Irrigation Management Information System (CIMIS) station #52 (https://cimis.water.ca.gov/Default.aspx), located 1 km from the experimental site.

2.2.8 Statistical analyses

All statistical analyses were conducted using JMP Pro 18 statistical software (SAS Institute Inc., Cary, NC). A split-plot analysis of variance (ANOVA) with RCBD was used to determine the significance of effects (treatment and cultivar) and their interaction on the differences of percent mortality, AUDPC, fruit yield, and salinity symptom assessments. Means were separated by Tukey honestly significant difference (HSD) separation of means. Pearson's correlation test was performed to evaluate the relationship among visual salinity symptom assessments and aerial imaging data.

2.3 Results

2.3.1 Plant mortality

Across both years of the study, symptoms of Macrophomina root rot were first observed in May, followed by a rapid increase in plant mortality during mid- to late-June. There was no significant treatment × cultivar interaction in 2024 or 2025 (P = 0.557 and 0.381, respectively). Treatment had a significant effect on final plant mortality across both years (P = 0.008 and P = 0.024 for 2024 and 2025, respectively). The average mortality of the standard treatment was 37.2% in 2024 and 19.9% in 2025. Disease incidence was significantly increased in the

drought stress treatment in 2024 and in the high EC_W stress in 2025 (Fig. 2.4). The average plant mortality of the chloride and chloride × 2 treatments were not significantly different from the standard either year. Cultivar had a significant effect on plant mortality within both years of this study ($P < 0.0001$ and $P < 0.0001$, respectively). 'Sweet Ann' had significantly higher rates of plant mortality than 'Fronteras' across both years (Fig. 2.5).

There was no significant interaction between treatment × cultivar for AUDPC in 2024 or 2025 ($P > 0.05$). Treatment had a significant effect on AUDPC across both years ($P = 0.0009$ and $P = 0.0236$, respectively). In 2024, AUDPC was significantly higher under drought stress in comparison to all other treatments, while in 2025 AUDPC was higher under high EC_W stress in comparison to the other treatments (Fig. 2.6). Across both years, cultivar had a significant effect on AUDPC ($P < 0.0001$ and $P < 0.0001$, respectively). Plots planted with 'Sweet Ann' exhibited higher AUDPC values than 'Fronteras' (Fig. 2.6).

2.3.2 Fruit yield

The observed fruit trends during the 2025 season closely aligned with the annual fruit volume trends for the Santa Maria district (CSC, 2024b), validating the selected production intervals used for the yield picks in 2024. In 2024 and 2025, there was no significant treatment × cultivar interaction on total marketable fruit yield ($P > 0.05$). In 2024, during the peak-season (May), the effect of stress treatment averaged across cultivars ($P = 0.809$) and cultivar ($P = 0.269$) on total marketable fruit yield was not statistically significant. During the late-season

(July), treatment (P = 0.021) and cultivar (P = 0.0005) had a significant effect on the total marketable fruit yield. Drought was the only stress treatment to significantly reduce marketable fruit yield (0.29 kg/m^2) compared to the standard treatment (0.57 kg/m^2; Fig. 2.7). Regardless of the stress treatment, 'Fronteras' had a significantly higher total marketable fruit yield than 'Sweet Ann' (Fig. 2.8).

In 2025, a significant difference in weekly marketable fruit yield between treatments was first observed on 23 June 2025 (Fig. 2.9). Both treatment (P = 0.012) and cultivar (P < 0.0001) had a significant effect on the end-of-season (7 March to 28 July), total marketable fruit yield. The drought and high EC_W stress resulted in a 13.3 and 16.1% reduction, respectively, in whole season yield compared to the standard treatment (Fig. 2.10). The total fruit yield of the chloride and chloride × 2 treatments were not significantly affected. 'Fronteras' produced significantly higher yields (24.8%) than 'Sweet Ann' (Fig. 2.11).

2.3.3 Salt stress symptom assessment

Visual assessment scores for necrosis and chlorosis were more severe in 2024 than 2025. When visually comparing the images of plants from both years of the experiment, the 2025 experiment plots appeared much fuller and darker green when than those in 2024. This is corroborated by the comparison of aerial imaging data from each year. Plants within the 2024 season had lower average LAI and NDRE values than those in 2025 (Table 2.3). There was no significant treatment × cultivar interaction for any of the salt stress symptom assessments in either year of the study (P > 0.05). No significant differences in necrosis or chlorosis severity scores were detected among treatments in either year of the

study ($P > 0.05$). The only significant differences in visual assessment scores were observed between cultivars in 2025, in which Sweet Ann exhibited greater levels of necrosis and chlorosis when compared to Fronteras. Using aerial imaging data, significant differences in LAI were observed between treatment ($P = 0.027$) and between cultivar only in 2025 ($P < 0.0001$; Table 2.3). Plants subjected to the high EC_W treatment in 2025 had significantly lower LAI values in comparison to the standard treatment. In 2025, higher average LAI values were observed for 'Fronteras' in comparison to 'Sweet Ann.' Across both years of the study, cultivar had a significant effect on NDRE ($P = 0.002$ and $P < 0.0001$, respectively), with Fronteras exhibiting higher NDRE scores than Sweet Ann.

Significant correlations between visual salinity symptom assessments and aerial imaging indices were identified in 2025 (Table 2.5), but not in 2024 (Table 2.4). In 2025, LAI and NDRE were weakly and negatively correlated with necrosis severity and moderately and negatively correlated with chlorosis severity.

2.3.4 Weather data

Monthly rainfall was higher and more frequent during the early season of the 2024 experiment, delaying the initial onset of stress treatments until mid-March (Fig. 2.12). Total precipitation throughout the season amounted to 57-cm in 2024 and 37-cm in 2025 season, representing a 20-cm difference in total rainfall between years. In terms of average monthly air and soil temperature, 2024 and 2025 were similar (Fig. 2.13).

2.4 Discussion

The results of this study suggest drought and high EC_W stress are major predisposing factors contributing to greater Macrophomina root rot incidence in strawberry. The findings of this study align with previous research demonstrating exposure to environmental stressors is associated with increased disease severity caused by *M. phaseolina* on other crops, including strawberry (Pedroncelli et al. 2025), sorghum (Goudarzi et al. 2011), soybean (Kendig et al. 2000), and common bean (You et al. 2011). In addition to the effect of treatment, differences in total plant mortality and AUDPC between cultivars was consistent with current literature stating that Sweet Ann is more susceptible to Macrophomina root rot than Fronteras (Wang et al. 2024).

Fruit yield was collected to assess the potential economic impacts that correlate with losses due to Macrophomina root. Within both years of the study, significant differences in overall fruit yield among treatments were not observed until the late-season harvests (June and July). The delay in salinity treatment effect may be explained by the heavy soil of experimental site, in which salts applied through irrigation water require longer time (compared to lighter soils) to accumulate in the soil exchangeable sites to levels that would induce earlier plant stress. The treatments that significantly reduced overall fruit yield included drought stress, across both years, and the high EC_W stress in 2025. Differences in the effect of high ECw between 2024 and 2025 could be explained by the fact that ECw in 2025 was 27% greater than 2024.

These results indicate that the use of cultural control strategies is paramount to reducing Macrophomina root rot disease progression and sustaining yields during the late-season harvest window. Strategies that growers can implement include maintaining optimal soil moisture levels using tensiometers (Pedroncelli et al. 2025), increasing the number of drip tape lines (Blauer and Holmes 2023), avoiding the use of poor-quality irrigation water when possible (Al-Shorafa et al. 2014), and planting disease-resistant varieties (Baggio et al. 2021a). When high-quality irrigation water is not available, it's important to apply sufficient irrigation to leach salts accumulating within the root zone and to avoid excessive fertilizer use, especially those high in soluble salts, which can further exacerbate issues of elevated salinity (Rhoades 1974).

Current literature states that a crucial step to identifying sources of resistance to Macrophomina root rot involves phenotypic screening under heat and drought stress (Knapp et al. 2024), suggesting that resistance is closely tied to a cultivar's ability to tolerate abiotic stresses. The results of this study indicate that the use of irrigation with elevated salinity influences disease development, highlighting salinity as a potential additional stress factor. Future work could therefore investigate whether phenotypic screening under saline conditions may also serve as a useful approach for identifying resistant cultivars.

Although the mortality rate and fruit yield of the chloride and chloride $\times$ 2 treatments did not separate from the standard treatment either year, limitations of this study must be considered. This experiment does not account for the salt accumulation within the soil that would normally occur when using irrigation water

with elevated salinity levels over multiple years. According to Ayers and Westcot (1985), when high-quality irrigation water is used without leaching, two or more consecutive years of irrigation are required to accumulate salts within the soil to levels that adversely affect crop yield. Although this experiment was conducted in the same location, disease response varied between the two years. Differences in disease response may be due to variations in environmental factors, aggressiveness of fungal isolates used (Avilés et al. 2009), or operational practices, such as changes in nitrogen fertilization. Average air and soil temperatures were similar across both years. However, the frequency of air temperatures recorded above 26°C differed. In 2024, seven days between June and August exceeded 26°C, whereas only a single day reached that threshold in 2025. Precipitation was another environmental factor distinguishing the two years, with the 2024 season receiving 20-cm more rainfall than 2025. The onset of treatment applications was delayed during the 2024 experiment, due to heavy rainfall, which therefore may have influenced disease incidence and percent mortality of stress treatments within the 2024 experiment.

Drone imagery was used as a tool for evaluating salt-related injuries present on plant foliage but showed mixed results across both years of this study. When compared to visual observations, LAI and NDRE had significant correlations to visual necrosis and chlorosis severity scores in 2025, but not 2024. Changes in fertilization practices across this two-year study may have influenced the severity of salinity symptoms. Plants within the 2025 experiment received higher rates of nitrogen throughout the fruiting season in order to

capture yield data that would be reflective of a grower's operation. This may indicate that drone imagery alone may not be a reliable indicator for evaluating salinity symptoms; at least not in the conditions of this study. This aligns with a study done by Ivushkin et al. (2019), which determined that multispectral vegetation indices relating to greenness or green biomass were not valuable indicators of salt stress in quinoa plants.

Table 2.3. Average necrosis score, chlorosis score, leaf area index (LAI), and normalized difference red-edge index (NDRE) of each treatment and cultivar in 2024 and 2025

		Necrosis		Chlorosis[a]		LAI		NDRE	
Factor	**Variable**	**2024**	**2025**	**2024**	**2025**	**2024**	**2025**	**2024**	**2025**
Treatment	Standard	24.50	8.63	22.38	6.00	1.17	2.51 a	0.15	0.32
	Chloride	27.75	9.50	26.00	6.63	1.13	2.42 ab	0.15	0.32
	Chloride × 2	29.50	11.75	17.25	7.13	1.11	2.39 ab	0.15	0.31
	High EC_W	28.00	11.50	21.75	6.13	1.12	2.21 b	0.15	0.30
	Drought	27.75	11.38	25.25	6.63	1.05	2.33 ab	0.14	0.32
Cultivar	Sweet Ann	27.20	11.35 a	22.05	9.55 a	1.11	2.13 b	0.14 b	0.29 b
	Fronteras	27.80	9.75 b	23.00	3.45 b	1.12	2.62 a	0.15 a	0.34 a

[a] Values not connected by the same letter are significantly different ($P < 0.05$).

Table 2.4. Correlation coefficients (*r*) among necrosis and chlorosis severity scores across leaf area index (LAI) and normalized difference red-edge index (NDRE) values from the 2024 experiment

	Necrosis	Chlorosis
LAI	0.04	-0.02
NDRE	0.08	-0.06

* Indicates *P* value < 0.05.

Table 2.5. Correlation coefficients (*r*) among necrosis and chlorosis severity scores across leaf area index (LAI) and normalized difference red-edge index (NDRE) values from the 2025 experiment

	Necrosis	Chlorosis
LAI	-0.42*	-0.66*
NDRE	-0.37*	-0.69*

* Indicates *P* value < 0.05.

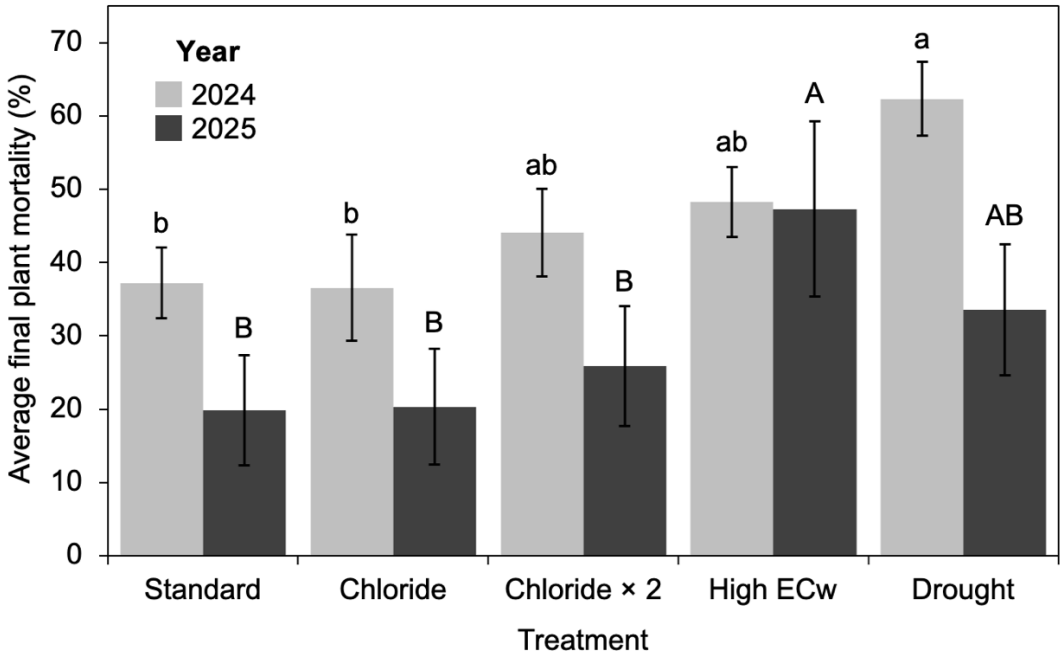

Figure 2.4. Average final plant mortality (%) of each treatment from 2024 and 2025. Values not connected by the same letter (and case) are significantly different ($P < 0.05$). Error bars represent the standard error of the means (n = 4).

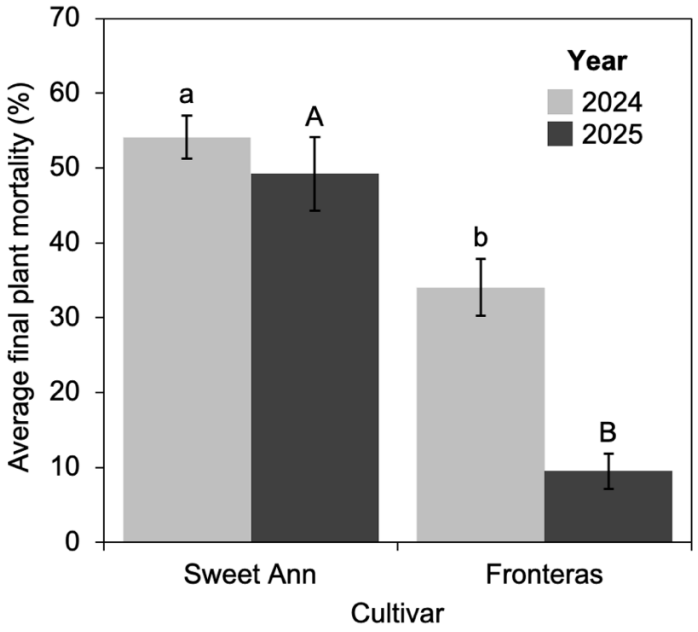

Figure 2.5. Average final plant mortality (%) of each cultivar from 2024 and 2025. Values not connected by the same letter (and case) are significantly different ($P < 0.05$). Error bars represent the standard error of the means (n = 4).

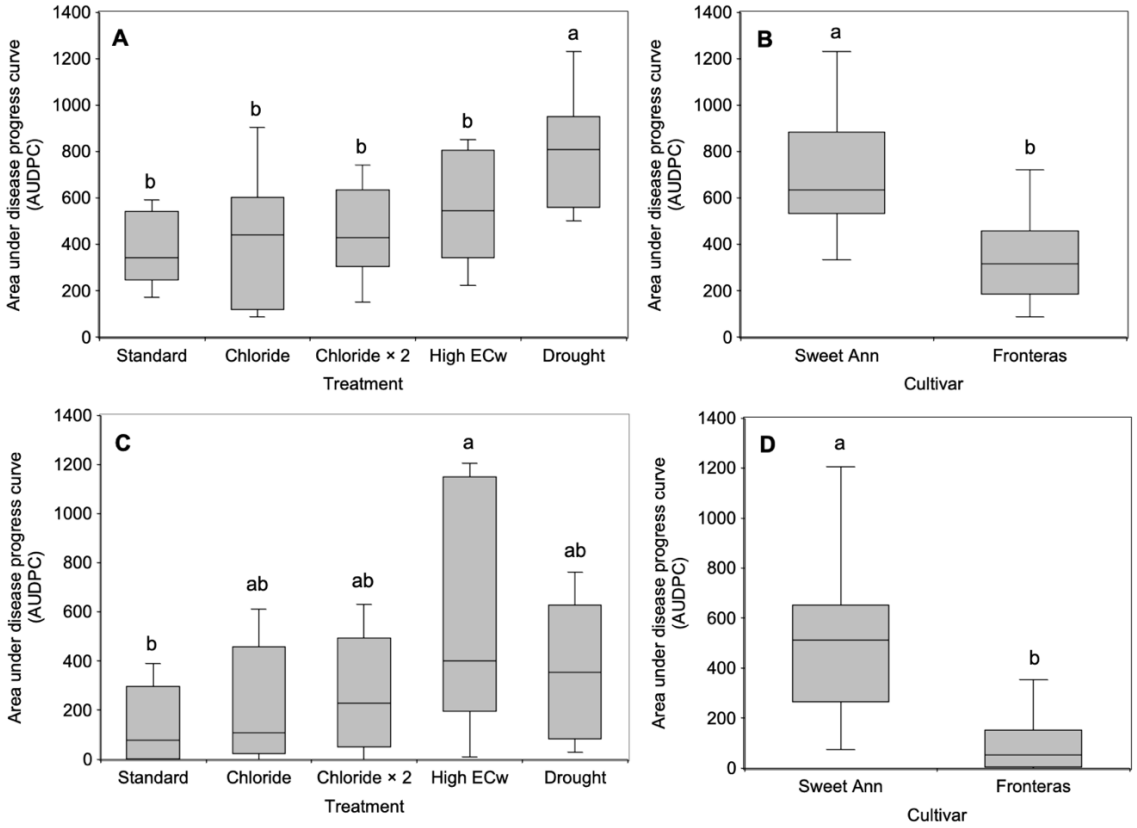

Figure 2.6. Area under the disease progress curve (AUDPC) in 2024: (A) treatment averaged across both cultivars, and (B) cultivar; and in 2025: (C) treatment averaged across both cultivars, and (D) cultivar. Values not connected by the same letter are significantly different ($P < 0.05$). Error bars represent the standard error of the means (n = 4).

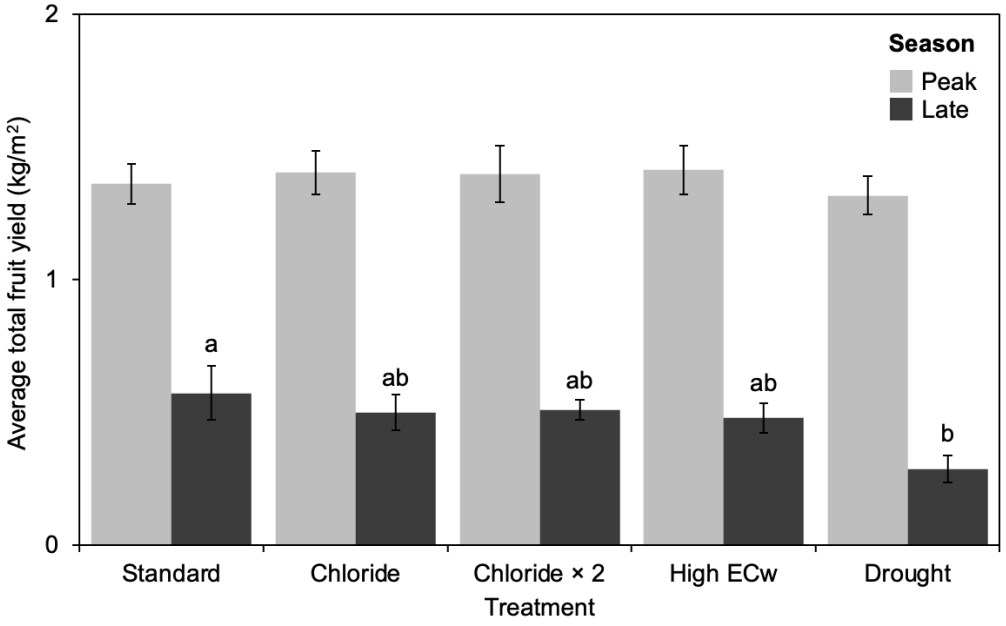

Figure 2.7. Average total marketable fruit yield (kg/m^2) of each treatment from harvest events during the peak-volume (May) and late-season (June) of 2024. Values not connected by the same letter are significantly different ($P < 0.05$). Error bars represent the standard error of the means (n = 4).

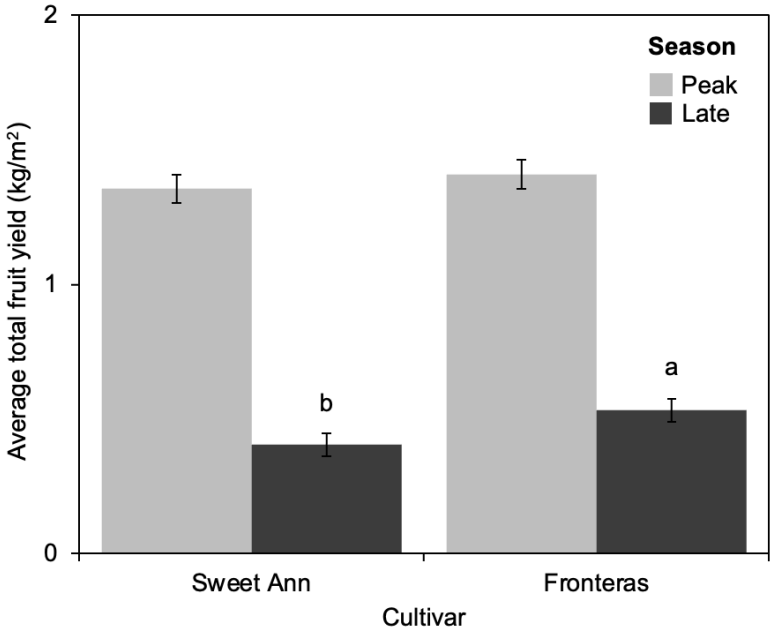

Figure 2.8. Average total marketable fruit yield (kg/m^2) of each cultivar from harvest events during the peak-volume (May) and late-season (July) of 2024. Values not connected by the same letter are significantly different ($P < 0.05$). Error bars represent the standard error of the means (n = 4).

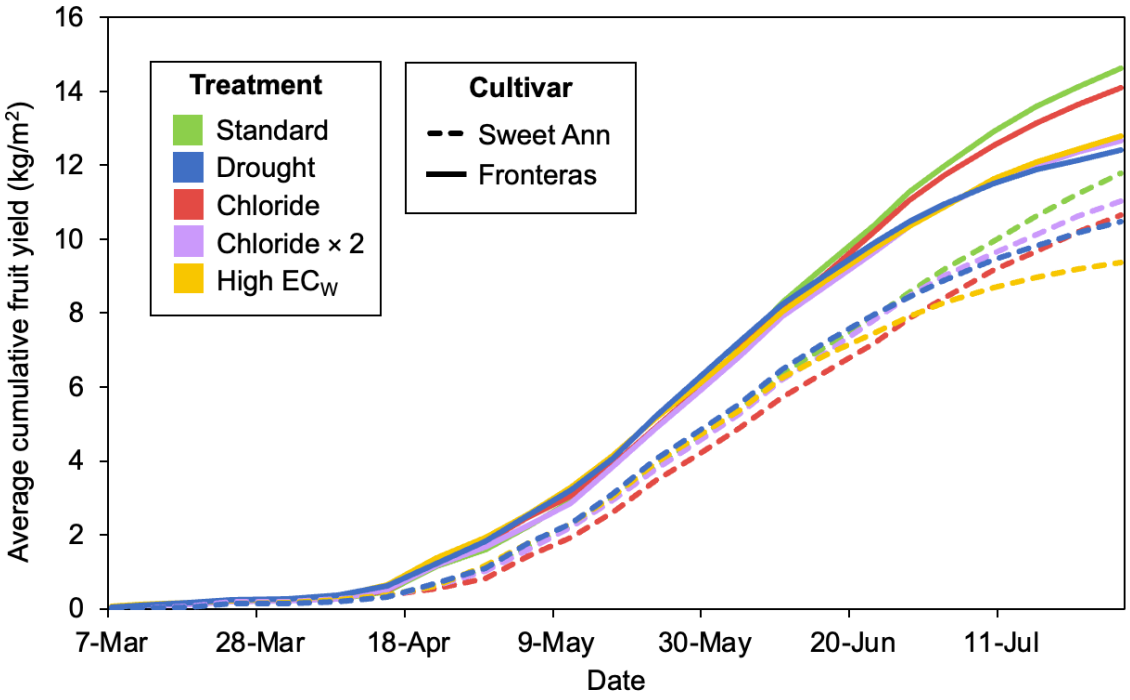

Figure 2.9. Timeline showing the cumulative fruit yield (kg/m^2) from 2025.

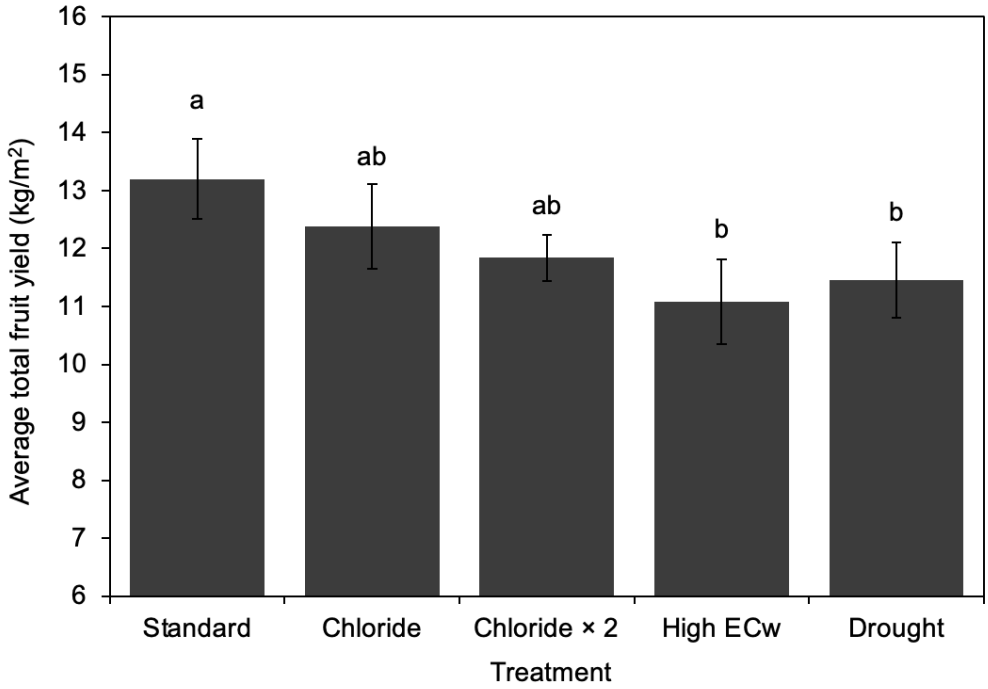

Figure 2.10. Average total marketable fruit yield (kg/m^2) of each treatment in 2025. Values not connected by the same letter are significantly different (P < 0.05). Error bars represent the standard error of the means (n = 4).

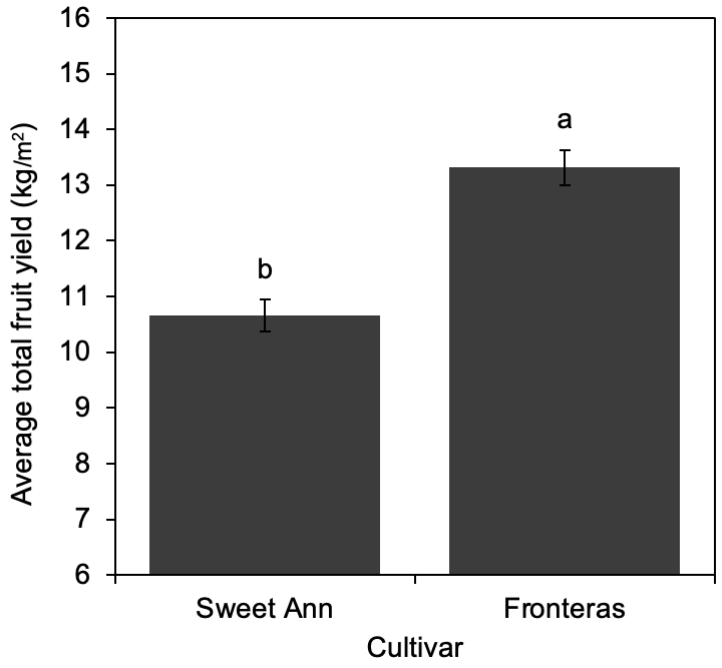

Figure 2.11. Average total marketable fruit yield (kg/m^2) of each cultivar in 2025. Values not connected by the same letter are significantly different ($P < 0.05$). Error bars represent the standard error of the means (n = 4).

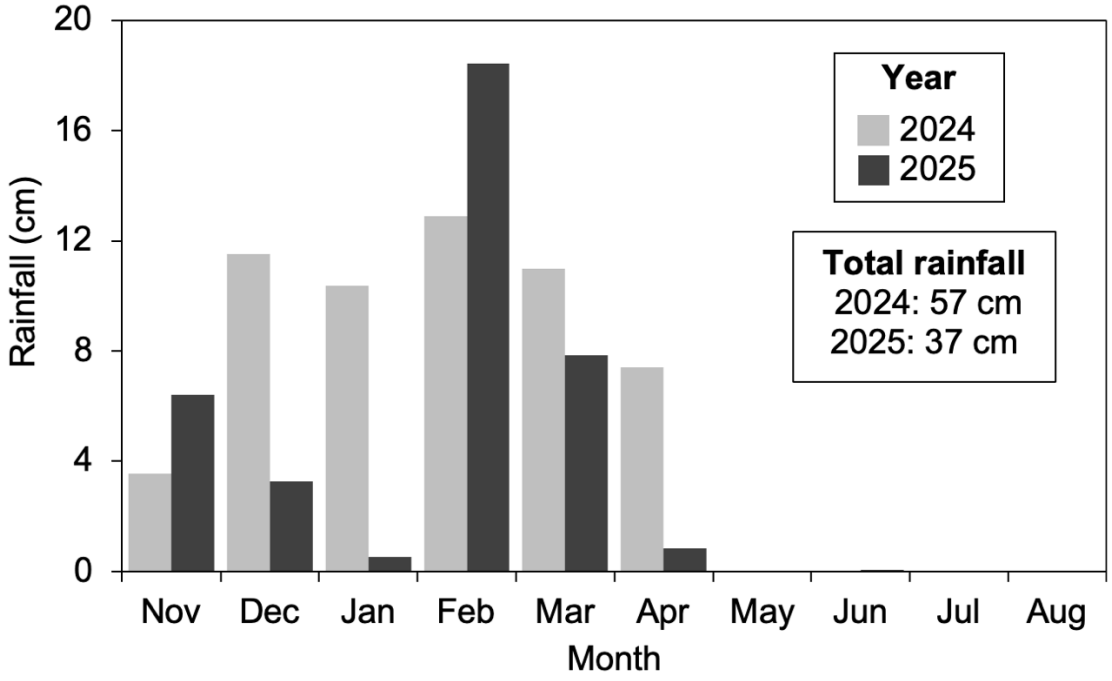

Figure 2.12. Total monthly rainfall (cm) in 2024 and 2025. Data were obtained from California Irrigation Management Information System (CIMIS) station #52.

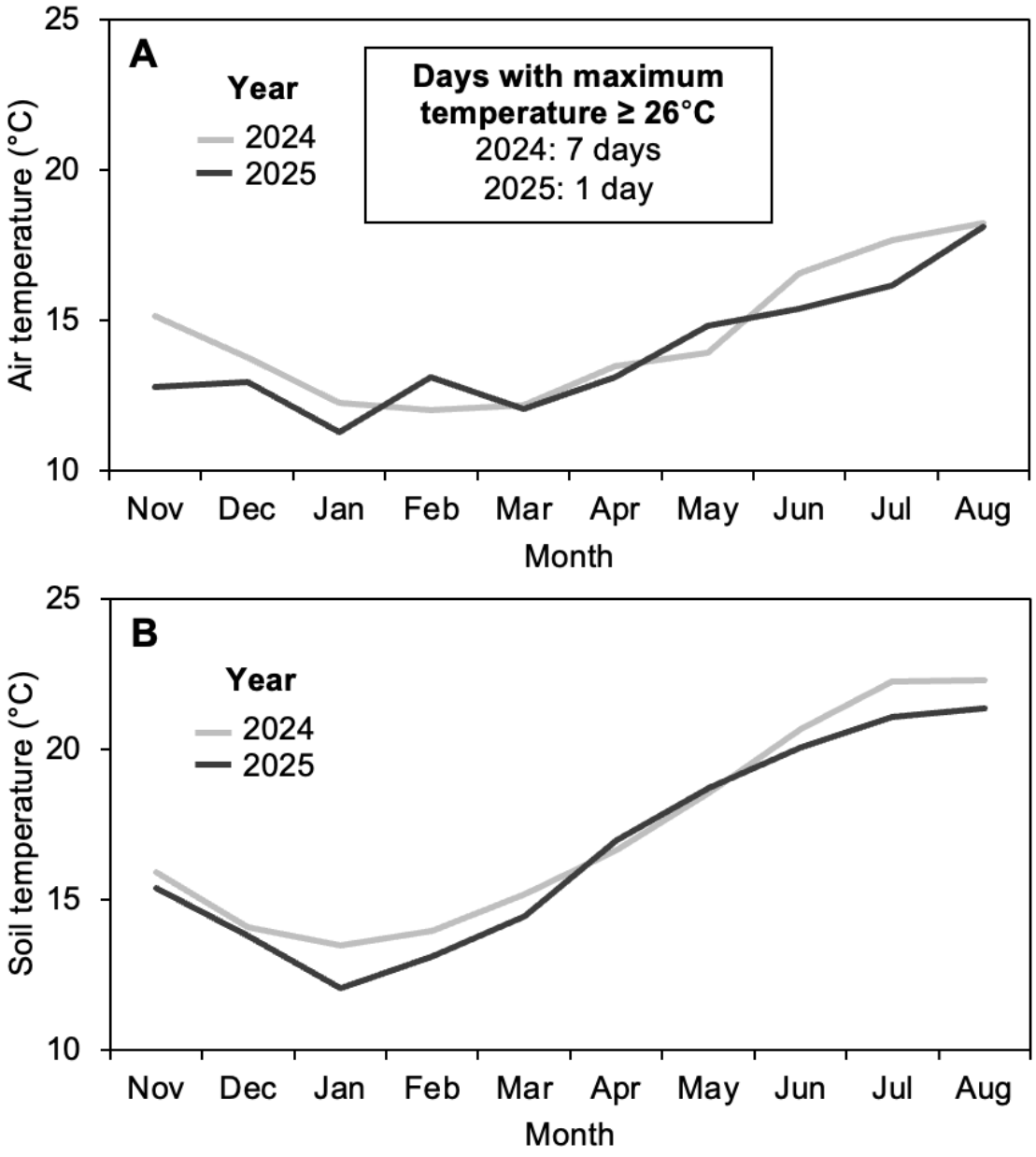

Figure 2.13. Monthly average (A) air and (B) soil temperature (°C) at a 15-cm depth in 2024 and 2025. Data were obtained from California Irrigation Management Information System (CIMIS) station #52.

Chapter 3

EFFICACY OF USING NANO-ENCAPSULATED CITRUS OILS TO CONTROL STRAWBERRY PATHOGENS CAUSING BOTRYTIS FRUIT ROT AND POWDERY MILDEW

3.1 Introduction

In 2023, the United States ranked as the second largest producer of strawberry worldwide, after China (FAO 2023). Within the US, California represents the vast majority of strawberry production, accounting for approximately 90%, and in 2024, strawberries were ranked as California's 4th highest grossing crop valued at $3.46 billion (CDFA 2024). The California strawberry industry continues to face significant crop losses caused by airborne pathogens that infect plant foliage and fruit. Currently, the most economically significant fruit disease is Botrytis fruit rot, while powdery mildew remains the most important foliar disease (Holmes 2024).

Botrytis fruit rot, caused by *Botrytis cinerea*, is considered the most destructive disease of strawberry fruit worldwide. The pathogen can infect fruit at all stages of production, including in-field and postharvest settings (Romanazzi et al. 2022; Romanazzi and Feliziani 2014). Early symptoms of Botrytis fruit rot appear as small brown lesions which expand and become covered with gray sporulating growth. *B. cinerea* has a wide range, with at least 200 susceptible plant hosts identified within current literature (Williamson et al. 2007). Powdery mildew, caused by *Podosphaera aphanis*, is also widespread within California production systems, with disease severity exacerbated in controlled

environments such as greenhouses and plastic tunnels (Xiao et al. 2001). Symptoms of powdery mildew appear as curling of the leaf margins and purple-red blotches on the lower leaf surface and signs of the pathogen will appear as white, powdery growth observed on leaves, petioles, and fruit (UC IPM 2018). Unlike *B. cinerea*, *P. aphanis* has a restricted host range and is only known to infect strawberry. Although cultural practices are utilized as important preventative measures, chemical fungicides remain the most common method for controlling both diseases as they are efficient, reliable, and economically effective (Mertely et al. 2000).

However, the rapid emergence and increasing prevalence of fungicide-resistant pathogen populations threaten the long-term efficacy of site-specific fungicides (Hahn 2024). *B. cinerea* is classified as an organism with a high risk of developing resistance and *P. aphanis* is considered a 'medium risk' organism (FRAC 2019; Hahn 2014). Isolates resistant to major site-specific chemical classes have been documented for both *B. cinerea* and *P. aphanis* across all major strawberry growing districts in California (Cosseboom et al. 2019; Palmer and Holmes 2021). This highlights the importance of researching and developing alternative control strategies that could reduce reliance on single-site fungicides and preserve their efficacy.

A promising alternative is the use of essential oils as biological control agents. Essential oils are categorized as Generally Recognized as Safe (GRAS) by the US Food and Drug Administration and exhibit broad antimicrobial activities (Callaway et al. 2011; El Asbahani et al. 2015). The use of citrus essential oils, in

particular, have gained significant interest due to the abundance of citrus peel waste generated within major citrus production regions, such as California, making them readily available and often at low-cost (Callaway et al. 2011). The main biologically active component of citrus essential oil is the compound known as *d*-limonene (Shehata et al. 2020), which is capable of inhibiting fungal pathogens by disrupting cell membrane and cell wall integrity, ultimately leading to cell lysis (Lin et al. 2024). Utilizing essential oils as a biological alternative to synthetic chemicals could help limit crop losses while also reducing fungicide use and slowing resistance development to major fungicide classes.

Despite these advantages, concerns related to low solubility, high volatility, and the risk of phytotoxicity to crop plants limit the practicality of using these products in commercial field settings (Donsí and Ferrari 2016; Werrie et al. 2020). Nano-encapsulation of essential oils offers a potential solution to the current limitations by enhancing solubility and retention of volatile compounds (Miastkowska et al. 2020). Recent studies revealed that nano-encapsulated celery seed oils demonstrated better control of the causal agent of cucumber powdery mildew when compared to the pure oil (Soleimani et al. 2023; Soleimani et al. 2024). A large majority of published research remains limited to *in vitro* or postharvest assays, necessitating a study to evaluate the efficacy of nano-encapsulated essential oils across a broader range of conditions. The objective of this study is to evaluate the efficacy of nano-encapsulated citrus essential oils for the control of *B. cinerea* and *P. aphanis* under *in vitro*, *in planta*, greenhouse, and field environments with the goal of gaining a more comprehensive

understanding of product efficacy, phytotoxicity potential, and practical feasibility in commercial production systems.

3.2 Materials and methods

3.2.1 Harvesting citrus

All citrus fruit were harvested from the California Polytechnic State University (Cal Poly) Crops Unit orchard in San Luis Obispo, CA (Fig. 3.1). The three citrus species with the highest global production volume were selected for this trial (Kale and Adsule 1995): 'Washington' navel oranges (*Citrus sinensis*), 'Clemenules' mandarins (*Citrus reticulata*), and 'Lisbon' lemons (*Citrus* × *limon*). Any ripe fruit that were misshapen or showing signs of rot or insect damage were discarded. Marketable ripe fruit were stored in a commercial cooler at 5°C until shipment. Citrus fruit were packaged and shipped to Virginia Polytechnic Institute and State University (Virginia Tech) in Blacksburg, VA, to be processed.

Figure 3.1. (A) Orange grove within the Cal Poly Crops Unit orchard. (B) Each fruit was harvested by hand, using Corona AG5050 shears (Corona Clipper Inc., Corona, CA). (C) Example of citrus fruit with no remaining vegetative material.

3.2.2 Essential oil extraction and encapsulation

This part of the method was carried out by food technologists at Virginia Tech University. In brief, the citrus peels were freeze-dried to remove water and ground into a fine powder using a hammer mill. The essential oils were extracted from the milled peel using an accelerated solvent extraction technique with 95% ethanol as the solvent, described by Vilas-Franquesa et al. (2022). The liquid extract was subjected to vacuum filtration and rotary evaporation to remove the solvent and insoluble impurities. The extracted oils were characterized using a gas chromatography mass spectrometry analysis and nano-encapsulated (L. Yang et al., *unpublished*).

While waiting for the nano-encapsulated essential oils from citrus harvested from Cal Poly, preliminary experiments were conducted using commercially available essential oils. Two types of essential oils were purchased: Orange oil (*Citrus sinensis*) (Wholesale Botanics Inc., Vancouver, WA) and lemon oil (*Citrus* × *limon*) (Wholesale Botanics Inc., Vancouver, WA). These products were nano-encapsulated at Virginia Tech for use in the preliminary trials and used as-is for comparison. Nano-encapsulated products were stored at 3°C in the absence of light in order maintain the products stability over time (Turek and Stintzing 2013).

3.2.3 Inoculum production of *Botrytis cinerea*

Three *Botrytis cinerea* isolates (Bc 40, Bc 44, and Bc 132) with no history of fungicide resistance, were used in this trial (Table 3.1). Isolates were thawed

from long-term, -80°C storage, plated on potato dextrose agar (PDA), and allowed to grow for 14 days at 23°C.

Table 3.1. *Botrytis cinerea* isolates used for the *in vitro* and detached fruit assays

Isolate	Date collected	Isolated from
Bc 40	23 Mar 2016	Salinas, CA
Bc 44	21 Mar 2016	Salinas, CA
Bc 132	23 Feb 2017	Unknown

A spore suspension was prepared by flooding 14-day-old plates of *B. cinerea* with 5 ml of sterile deionized water containing Tween 20 (0.1 ml/liter water). The fungal growth was disrupted using a sterile glass rod and the resulting spore suspension was filtered through four layers of cheesecloth. Spore concentration was determined using a hemocytometer (Hausser Scientific, Horsham, PA) and the final concentration was adjusted to 1×10^6 spores/ml. Spore suspensions of the three isolates were combined into a single spore suspension.

3.2.4 *In vitro* assay for *Botrytis cinerea*

To make infested agar plugs, 1 ml of the *B. cinerea* spore suspension was applied to the surface of a Petri plate containing PDA. A 5 mm cork borer was used to cut agar plugs. On a separate Petri plate containing PDA, 100 µl of a treatment solution (Table 3.2) was applied and spread across the medium surface using a sterile glass rod. One infested agar plug was placed in the center of each treated plate, surface-down to ensure spores made contact with the treatment, and plates were incubated at 23°C for 4 days. After incubation, the

colony diameter was measured, and percent inhibition was calculated using the following equation:

$$\%\ \text{inhibition} = \frac{(\bar{X} - X_i)}{\bar{X}} \times 100$$

$\bar{X}$ represents the mean colony diameter on non-treated PDA (minus the 5 mm inoculum plug) and X_i represents the mean colony diameter on treated PDA (minus the 5 mm inoculum plug).

Table 3.2. List of treatments for *in vitro* assay for *Botrytis cinerea*

Treatment	Active ingredient	Active ingredient % by weight	FRAC code	Concentration
non-treated control	-	-	-	-
Miravis Prime	pydiflumetofen + fludioxonil	12.8, 21.4	7 + 12	0.677 ml/liter
Captan	captan	80	M4	2.996 mg/liter
Oso	polyoxin D	5	19	0.677 ml/liter
Prev-Am	sodium tetraborohydrate decahydrate	0.99	IRAC 8D	3.91 ml/liter
nano-encapsulated orange oil (NEO)[a]	nano-encapsulated orange oil	10	NC	0.5, 1, 3, and 4% ai (v/v)
nano-encapsulated lemon oil (NEL)[a]	nano-encapsulated lemon oil	10	NC	0.5, 1, 3, and 4% ai (v/v)

[a] Commercially available essential oil (Wholesale Botanics Inc., Vancouver, WA).

3.2.5 Detached fruit bioassay for Botrytis fruit rot

Pink ‘Fronteras’ strawberries were harvested from field 35b at Cal Poly. Pink fruit were defined as fruit showing the initial change in color from white to pink. Detached fruit were surface sterilized in 0.5% NaClO for 3 min and rinsed with deionized water three times. After sterilization, fruit were dipped into a treatment (Table 3.3; Fig. 3.2) for 1 s and placed onto a paper towel to air dry.

Table 3.3. List of treatments used in detached fruit bioassay for Botrytis fruit rot

Treatment	Active ingredient	Active ingredient % by weight	FRAC code	Concentration
non-treated control	-	-	-	-
Miravis Prime	pydiflumetofen + fludioxonil	12.8, 21.4	7 + 12	0.677 ml/liter
Captan	captan	80	M4	2.996 g/liter
Oso	polyoxin D	5	19	0.677 ml/liter
Prev-Am	sodium tetraborohydrate decahydrate	0.99	IRAC 8D	3.91 ml/liter
nano-encapsulated orange oil (NEO)[a]	nano-encapsulated orange oil	10	NC	0.5, 1, 3, and 4% ai (v/v)
orange oil[a] + Tween 80[b]	orange oil	100	NC	0.5, 1, 3, and 4% ai (v/v)

[a] Commercially available essential oil (Wholesale Botanics Inc., Vancouver, WA).
[b] Tween 80 was added as an emulsifier at 0.1%.

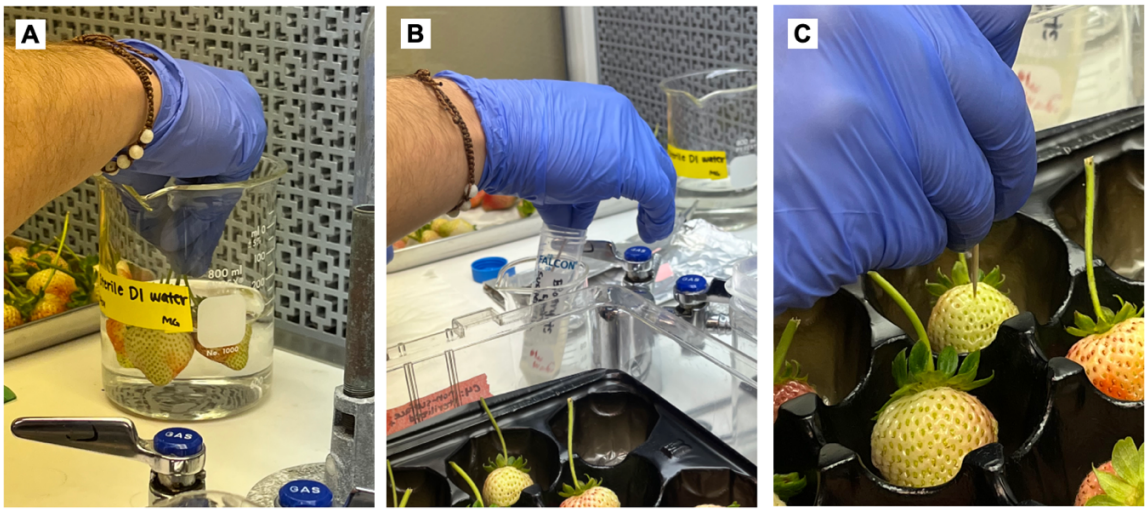

Figure 3.2. Detached fruit bioassay process. (A) Pink strawberries were dipped into a treatment for 1 s and allowed to air-dry. (B) A sterile toothpick was dipped into the *Botrytis cinerea* spore suspension and (C) used to inoculate treated fruit by wounding to a 2 mm depth.

Once dry, fruit were placed into a plastic container lined with polypropylene fruit trays. Empty tray wells were filled with sterile deionized water to maintain a high relative humidity conducive to disease development. To inoculate the fruit, a spore suspension was prepared as previously described. A sterile toothpick was dipped into the spore suspension and used to wound the fruit at a depth of 2 mm (Fig. 3.2). Each treatment was applied to five fruit and this was repeated three times. Infected fruit were incubated at room temperature (23 ± 2°C) for 4 days, after which disease incidence and percent inhibition were evaluated. Disease incidence was defined as the percentage of fruit with a visible lesion caused by *B. cinerea*. Disease inhibition was quantified by measuring the diameter of the lesion and calculating the percent inhibition using the following equation:

$$\%\ \text{inhibition} = \frac{(\bar{Y} - Y_i)}{\bar{Y}} \times 100$$

$\bar{Y}$ represents the mean lesion diameter on non-treated fruit and Y_i represents the mean lesion diameter on treated fruit.

3.2.6 In-field Botrytis fruit rot evaluation

This experiment was conducted in field 35b at Cal Poly. Bare-root 'Fronteras' transplants were planted on 31 October 2024. The experimental area consisted of four industry-standard raised beds, 45 m-long and 1.1 m-wide. The treatment plots were assigned according to a randomized complete block design with four replicates. Treatment plots contained 62 plants and were 6 m-long. A 1.5 m planted buffer was established on each end of the treatment plots to account for potential treatment spray overlap. For irrigation, three rows of high-flow drip tape (Toro, Bloomington, MN) (2.73 liter/min at 8 psi, 20 cm spacing between emitters) were laid 2.5 cm below the soil surface of raised beds.

New blooms were tagged with flagging tape prior to the first spray to track fruit development throughout the trial. All developing fruit beyond the flowering stage, prior to the first spray, were removed. Treatments were applied using a backpack sprayer equipped with a 1 m handheld boom (R&D Sprayers, Opelousas, LA). The boom consisted of eight hollow cone nozzles (Kisco Sales, Santa Maria, CA) spaced 30 cm apart and calibrated to deliver 1685 liters/ha (150 gal/A) using compressed CO_2 at 60 psi. The two outer nozzles were angled inward at 45° and the six inner nozzles were arranged in pairs, facing forward-backwards, at opposing 45° angles. Spray treatments (Table 3.4) began 23 April 2025 and were applied weekly for five consecutive weeks.

Table 3.4. List of treatments for the in-field Botrytis fruit rot trial

Treatment	Active ingredient	Active ingredient % by weight	FRAC code	Rate
non-treated control	-	-	-	-
Miravis Prime	pydiflumetofen + fludioxonil	12.8, 21.4	7 + 12	13.4 fl oz/A
Oso	polyoxin D	5	19	13 fl oz/A
greEnCap	encapsulated essential oils	100	NC	2% v/v
nano-encapsulated orange oil (NEO)[a]	nano-encapsulated orange oil	10	NC	1% ai (v/v)
orange oil[a] + Tween 80[b]	orange oil	100	NC	1% ai (v/v)
lemon oil[a] + Tween 80[b]	lemon oil	100	NC	1% ai (v/v)

[a] Commercially available essential oil (Wholesale Botanics, Inc. Vancouver, WA).
[b] Tween 80 was added as an emulsifier at 0.1%.

Once the tagged fruit within the trial reached full ripeness, evaluations for Botrytis fruit rot incidence were conducted at-harvest and postharvest to assess treatment efficacy. For the at-harvest evaluation, all ripe fruit were harvested from each plot, counted, and visually inspected for signs of infection by *B. cinerea*. Disease incidence was calculated by dividing the number of fruit infected with *B. cinerea* by the total number of fruit harvested from one plot. From each plot, 32 marketable fruit were selected for the postharvest evaluation and stored at room temperature (23 ± 2°C) in polypropylene stone fruit liners. During the postharvest evaluation, fruit were visually inspected daily, for eight days. Fruit

showing signs of infection were recorded and discarded to prevent the spread of disease from fruit-to-fruit. Area under the disease progress curve (AUDPC) was calculated for the disease incidence values of postharvest decay over time, using the following formula (Jeger and Viljanen-Rollinson 2001):

$$\text{AUDPC} = \sum_{i=1}^{N_{i-1}} \frac{(y_i + y_{i+1})}{2} \times (t_{i+1} - t_i)$$

N represents the total number of observations, y_i is the percent incidence for the observation number, and t_i represents the number of days from the planting date. This experiment will be repeated during the spring of 2026.

3.2.7 Weather data collection

Average rainfall, air temperature, and humidity were obtained from the California Irrigation Management Information System (CIMIS) station #52 (https://cimis.water.ca.gov/Default.aspx), located 1 km from the experimental site.

3.2.8 Detached leaflet bioassay for powdery mildew

Inoculation of *Podosphaera aphanis* was adapted from Asalf et al. (2012) and described by Palmer and Holmes (2021). Young, unexpanded 'Monterey' leaflets were collected from strawberry fields at Cal Poly. Young leaflets were used because they are most susceptible to infection by *P. aphanis* (Asalf et al. 2016) and 'Monterey' is a susceptible cultivar (Palmer and Holmes 2022). Petioles were removed and leaflets were surface sterilized in 0.5% NaClO with Tween 20 (0.1 ml/liter) for 3 min, rinsed in deionized water, and air-dried. Sterilized leaflets were dipped in a treatment (Table 3.5) for 1 s, three times in close succession, and placed onto a paper towel to dry. After air-drying, leaflets

were placed onto Petri plates containing water agar (5 g/liter) amended with benzimidazole (0.03 g/liter) to prevent contamination by other fungi and prolong longevity of the leaflets. A Petri plate containing three leaflets served as one replicate and was repeated three times.

For *P. aphanis* inoculum, leaves showing signs of powdery mildew were collected from greenhouse-grown strawberry at Cal Poly. Infected leaves were brought to the lab the same day as inoculation to ensure pathogen viability. Treated leaflets were transferred from the water agar medium to an Andersen sampler (Andersen 1958) and a camelhair brush was used to transfer a sporulating colony, 2-cm in diameter, of *P. aphanis* from the infected leaves onto one replication of treated leaflets (Fig. 3.3). A vacuum pump connected to the Andersen sampler was used to draw spores from infected leaves and uniformly spread these spores onto the treated leaflets. The treated and inoculated leaflets were placed back onto the water agar medium and stored in a growth chamber (Controlled Environments Inc., Pembina, ND) at 20°C and 16/8 h light/dark for 14 days. Three plates of non-inoculated leaflets served as a negative control to ensure there was no cross-contamination between treatments.

Table 3.5. List of treatments for detached leaflet bioassay for powdery mildew

Treatment	Active ingredient	Active ingredient % by weight	FRAC code	Concentration
non-treated control	-	-	-	-
Luna Sensation	fluopyram + trifloxystrobin	21.4, 21.4	7 + 11	0.396 ml/liter
Miravis Prime	pydiflumetofen + fludioxonil	12.8, 21.4	7 + 12	0.677 ml/liter
Microthiol Disperss	sulfur	80	M2	7.99 g/liter
nano-encapsulated orange oil (NEO)[a]	nano-encapsulated orange oil	10	NC	0.5, 1, 3, and 4% ai (v/v)
nano-encapsulated lemon oil (NEL)[a]	nano-encapsulated lemon oil	10	NC	0.5, 1, 3, and 4% ai (v/v)
orange oil[a] + Tween 80[b]	orange oil	100	NC	0.5% ai (v/v)
lemon oil[a] + Tween 80[b]	lemon oil	100	NC	0.5% ai (v/v)

[a] Commercially available essential oil (Wholesale Botanics Inc., Vancouver, WA).
[b] Tween 80 was added as an emulsifier at 0.1%.

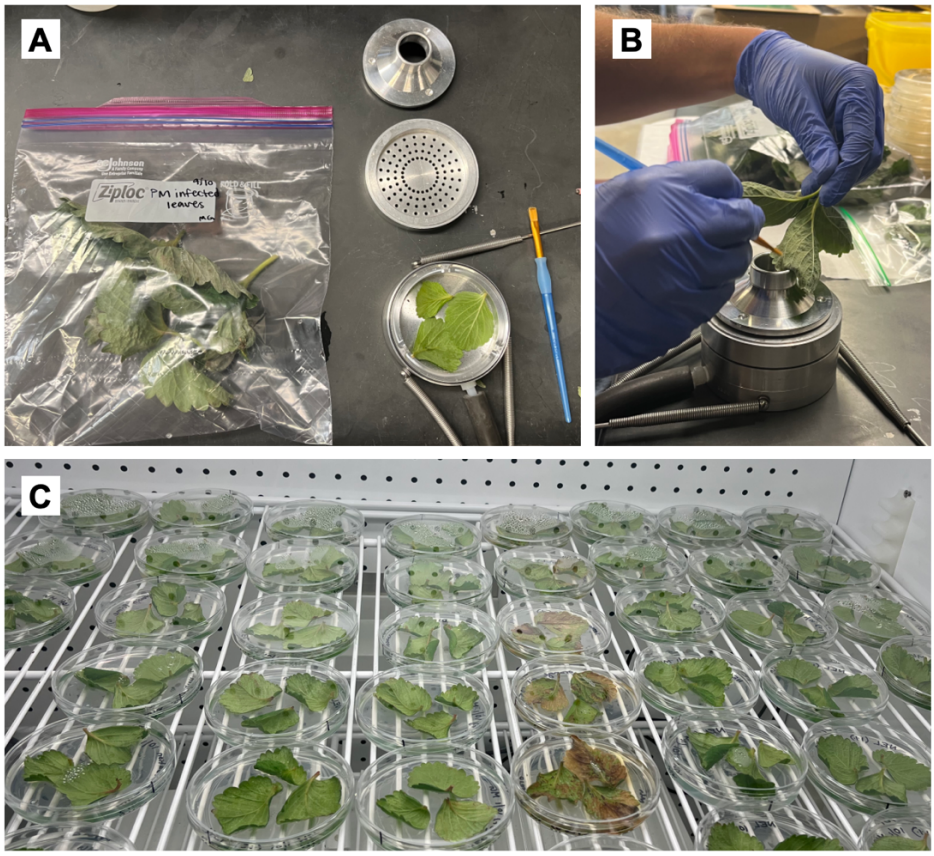

Figure 3.3. (A) Supplies for powdery mildew detached leaflet inoculation: leaves infected with *Podosphaera aphanis*, an Andersen sampler with treated leaflets, and a camelhair brush. (B) A sporulating lesion, roughly 2-cm in diameter, was brushed onto treated leaflets. (C) Treated and inoculated leaflets were incubated in a growth chamber at 20°C and 16/8 h light/dark for 14 days.

After incubation, disease incidence and severity was evaluated using a dissecting microscope at 5× magnification. Disease incidence was defined as the percentage of leaflets with at least one sporulating colony of *P. aphanis*. Disease severity was quantified as the percentage of the abaxial leaflet surface covered with visible sporulating colonies, adapted from Morishita et al. (2003). Each leaflet was assigned a score between 0 and 4: 0 = no visual infection, 1 = 0% to 5%, 2 = 5% to 25%, 3 = 25% to 50%, and 4 = >50% of the leaf surface covered in sporulating colonies (Fig. 3.4).

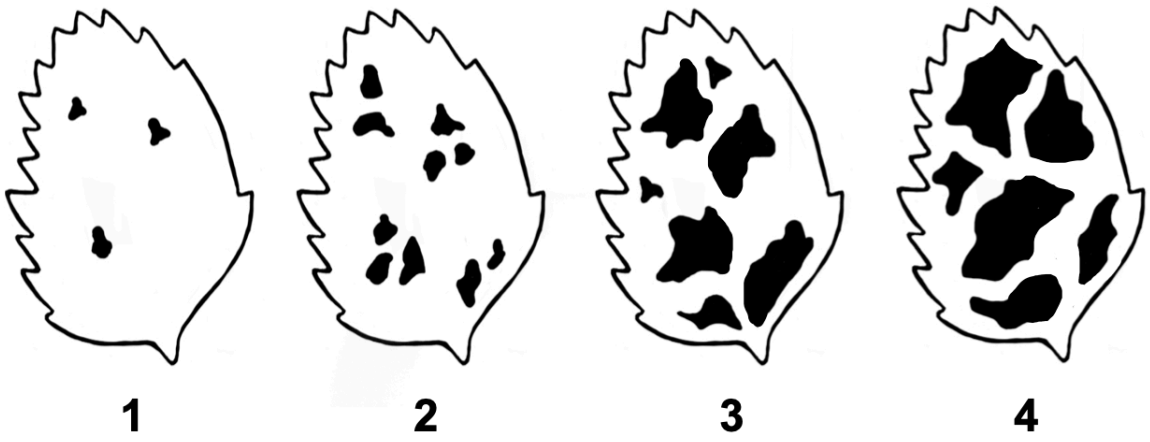

Figure 3.4. Powdery mildew severity scale (1-4) for detached leaflet bioassay.

3.2.9 Greenhouse powdery mildew evaluation

This experiment will be conducted in a greenhouse at the Cal Poly Crops Unit. Bare-root ‘Monterey’ transplants were planted on 30 October 2025, on outdoor raised nursery benches, into 3-liter plastic nursery pots (Greenhouse Megastore, Sacramento, CA) containing a soilless mixture called CB 1294 (Sun Gro Horticulture, Nipomo, CA). After establishing for two weeks, 10 g of Osmocote Plus (Scotts, Marysville, OH) was added to the soil surface. At the three-week mark, disease-free plants were moved into the greenhouse containing mature plants infected with a naturally occurring *P. aphanis* colony. Plants were arranged on greenhouse benches into treatment plots consisting of four pots (1 plant/pot). Plots were assigned according to a randomized complete block design with four replications. Stolons and fully ripe fruit were removed from plants weekly.

Treatments were applied using a backpack sprayer equipped with a single flat fan nozzle (DG8002VS yellow) (TeeJet Technologies, Clovis, CA) angled

down at 90° and calibrated to deliver 1124 liters/ha (100 gal/A) using compressed CO_2 at 35 psi. Spray treatments (Table 3.6) began four weeks after the initial planting date and were applied weekly for five consecutive weeks.

Table 3.6. List of treatments for the greenhouse powdery mildew trial

Treatment	Active ingredient	Active ingredient % by weight	FRAC code	Rate
non-treated control	-	-	-	-
Luna Sensation	fluopyram + trifloxystrobin	21.4, 21.4	7 + 11	0.396 ml/liter
Miravis Prime	pydiflumetofen + fludioxonil	12.8, 21.4	7 + 12	0.677 ml/liter
Microthiol Disperss	sulfur	80	M2	7.99 g/liter
nano-encapsulated orange oil (NEO)[a]	nano-encapsulated orange oil	10	NC	1 and 3% ai (v/v)
nano-encapsulated lemon oil (NEL)[a]	nano-encapsulated lemon oil	10	NC	1 and 3% ai (v/v)

[a] Commercially available essential oil (Wholesale Botanics Inc., Vancouver, WA).

One day prior to each spray application and two weeks after the final spray, leaf counts (number of leaves per plant), disease incidence, and disease severity were assessed. Disease incidence was defined as the percentage of trifoliate leaves with at least one visible powdery mildew lesion. Disease severity was assessed as the percentage of total leaf area, of fully emerged leaves, covered with visible mycelial growth. Each trifoliate leaf received a severity score

between 0 and 100: 0 = no visual infection and 100 = 100% of the leaf area is colonized by *P. aphanis*. Each side of the leaf (abaxial and adaxial) equated to 50% of the total leaf area. The severity scores from plants within one plot were averaged.

3.2.10 Statistical analyses

Statistical analyses were conducted using JMP Pro 18 statistical software (SAS Institute Inc., Cary, NC). A one-way analysis of variance (ANOVA) was used to determine the significance of fungicide treatments on disease incidence, disease severity, percent inhibition, and observed phytotoxicity. Means were separated by Tukey honestly significant difference (HSD) separation of means. For the greenhouse trial data, Fisher's LSD mean separation will be calculated with ARM version 2024 (GDM Solutions Inc., Brookings, SD).

3.3 Results

3.3.1 *In vitro* assay for *Botrytis cinerea*

Treatment had a significant effect on the percent inhibition of *B. cinerea* ($P < 0.0001$). None of the concentrations of nano-encapsulated orange oil (NEO) or nano-encapsulated lemon oil (NEL) resulted in inhibition levels that were significantly different from the non-treated control (Fig. 3.5). The only treatments that resulted in significantly increased inhibition of *B. cinerea* were the commercially available fungicides including Oso, Prev-Am, Captan, and Miravis Prime (Fig. 3.5). Both Captan and Miravis Prime resulted in the complete inhibition of *B. cinerea*, whereas the observed inhibition of Oso was 44.7% and Prev-Am was 68.1%.

3.3.2 Detached fruit bioassay for Botrytis fruit rot

In the trial comparing concentrations of pure orange oil, treatment had a significant effect on percent inhibition of *B. cinerea* ($P < 0.0001$). Orange oil applied at a 3% concentration, with the addition of Tween 80, significantly increased the percentage of inhibition compared to the non-treated control (Fig. 3.6). The inhibition observed in all other treatments resulted in no difference from the non-treated control (Fig. 3.6). Botrytis fruit rot incidence was observed at 100% occurrence across all treatments (data not shown).

In the trial comparing concentrations of NEO and Miravis Prime, treatment had a significant effect on both percent inhibition and incidence of *B. cinerea* ($P < 0.0001$ and $P < 0.0001$, respectively). The treatments that resulted in significantly increased inhibition of *B. cinerea* on detached fruit included NEO treatments applied at 3 and 4% concentrations and Miravis Prime (Fig. 3.7). Miravis Prime was the only treatment to significantly reduce Botrytis fruit rot incidence, with an average disease incidence of 6.7% in comparison to the 100% incidence observed in the non-treated control (Fig. 3.8).

3.3.3 In-field Botrytis fruit rot evaluation

Treatment did not have a significant effect on disease incidence at the in-field evaluation ($P = 0.1048$). Disease incidence at the in-field evaluation was extremely low with the highest average incidence rate of 0.03%, which was observed in the orange oil treatment (Fig. 3.9).

The postharvest evaluation at four days after harvest offered the most separation among treatments and revealed that treatment had a significant effect

on disease incidence ($P < 0.0084$). The treatment resulting in the highest disease incidence was lemon oil applied at a 1% concentration resulting in 39.8% incidence, followed by the non-treated control at 34.4%. Miravis Prime was the only treatment to significantly reduce Botrytis fruit rot disease incidence from the non-treated control in the postharvest evaluation (Fig. 3.9). Treatment also had a significant effect on AUDPC of Botrytis fruit rot incidence according to the postharvest evaluation ($P = 0.0002$). The only treatment with a significantly lower AUDPC than the non-treated control was the Miravis Prime treatment (Fig. 3.10). The AUDPC of the essential oil treatments, both pure and nano-encapsulated, and the organic products did not separate from the non-treated control.

3.3.4 Weather data

Over the length of the in-field Botrytis fruit rot trial, 0.79 cm of rainfall was received, with a majority of this rainfall occurring on one day (27 April 2025; Fig. 3.11). The average daily temperature throughout the trial was 14.1°C and the average relative humidity was 74.3% (Fig. 3.11).

3.3.5 Detached leaflet bioassay for powdery mildew

Treatment had a significant effect on the percent incidence of *P. aphanis* and on observed phytotoxicity ($P = 0.0178$ and $P < 0.0001$, respectively). In contrast, disease severity was not significantly affected by treatment ($P = 0.0552$).

Although treatment had a significant effect on percent incidence, pairwise comparisons revealed no significant differences were observed between individual treatments (Fig. 3.12). The non-treated control exhibited an average

disease incidence of 55%, whereas both Miravis Prime and Luna Sensation achieved complete inhibition of *P. aphanis*. All negative control leaflets (non-inoculated) showed no signs of infection. As with disease incidence, ratings of disease severity did not significantly differ between treatments (Fig. 3.13). The average disease severity across all treatments was relatively low, with the non-treated control receiving an average severity score of 1.2. Observed symptoms of phytotoxicity was significantly greater in the pure oil treatments, orange and lemon, applied at a 0.5% concentration (Fig. 3.14). Phytotoxic symptoms were also observed across a majority of the NEO and NEL concentrations, as well as in the Microthiol Disperss treatment, though they were not significantly different from the non-treated control (Fig. 3.14). In contrast, Miravis Prime and Luna Sensation did not result in any level of observed phytotoxicity.

3.4 Discussion

All data collected thus far are preliminary as the citrus oil extracts from citrus harvested at Cal Poly have not yet been nano-encapsulated and evaluated for efficacy. Although the essential oils from the same plant species (lemon and orange) will be evaluated, the chemical composition can be highly variable depending on culture site, growing conditions, and harvest timing, meaning that variations in efficacy between the commercial and Cal Poly products are likely (Santos-Gomes and Fernandes-Ferreira 2001).

The reduced efficacy observed between the detached fruit bioassay and *in vitro* assay against *B. cinerea* is possibly due to degradation of the nano-encapsulated product over time. The nano-encapsulated orange oil was first

received on 18 May 2025, used in the detached fruit bioassay on 3 June 2025, and evaluated for the *in vitro* assay on 5 November 2025. Over the five-month period, it is highly plausible that the product lost volatile compounds (Gago et al. 2019). Gago et al (2019) demonstrated that nano-emulsions progressively decrease in stability and antimicrobial activity over a six-month storage period at both 1 and 21°C, with degradation occurring more rapidly at higher temperatures. The food technologists at Virginia Tech will be evaluating the stability of the nano-encapsulated oil products over a 30-day period. However, it would be highly valuable to quantify the products stability over longer periods of time that would be more representative of the shelf-life requirements in agricultural settings.

The start of the in-field Botrytis fruit rot trial was pushed back due to delays in obtaining the nano-encapsulated product. There was little to no disease incidence at the in-field evaluation, placing a larger emphasis on the results of the postharvest assessment (Fig. 3.9). Although the air temperature and relative humidity levels throughout the duration of the trial were considered conducive to disease development of *B. cinerea* (Jarvis 1962), the limiting factor appeared to be leaf wetness duration as there was little precipitation during that period (Fig. 3.11). This experiment will be repeated earlier in the season of next year in order to capture disease incidence when environmental conditions are more conducive for *B. cinerea*.

Varying rates of phytotoxicity were observed throughout the duration of this experiment, in the detached fruit bioassay and in-field trial, prompting the

introduction of the phytotoxicity rating scale utilized in the detached leaflet bioassay. In the detached fruit bioassay, symptoms of phytotoxicity appeared in both the pure and nano-encapsulated essential oil treatments. Symptoms observed included the yellowing of fruit and necrosis of the fruit calyx, resulting in a “burned” appearance. This is consistent with a similar study by Soleimani et al. (2024), in which phytotoxicity was observed on the foliage of cucumber when applications of pure oil and nano-encapsulated oil were made. Within the in-field trial, phytotoxic symptoms appeared as small necrotic spots on foliage. These symptoms occurred most frequently in the pure oil treatment plots and tended to be more severe towards at the ends of plots. The higher incidence of phytotoxicity at the end of treatment plots is likely due to the overlapping applications at the plot borders. No phytotoxic symptoms were observed on developing fruit in the in-field trial.

Overall, the results of this study reveal both potential opportunities and key limitations associated with utilizing nano-encapsulated citrus oils for control of *B. cinerea* and *P. aphanis*. Nano-encapsulation offers several potential advantages, with opportunities such as providing a safer alternative to the use of conventional synthetic products for fungicide applicators, improving to the dispersibility of essential oils in aqueous solutions, and providing organic production systems with more options for disease control (Ali et al. 2017).

The current limitations include the product degradation over time, the low concentration of active ingredient present in the nano-encapsulated product, and concerns of phytotoxicity to crop plants. Considering that commercially available

fungicides are shelf-stable for multiple years, formulations that lose stability and efficacy over relatively short storage periods would likely be considered inadequate. Additionally, the current formulation of the nano-encapsulated product consists of 1% emulsifier, 10% essential oil, and 89% water. To achieve the target concentration of active ingredient for the efficacy trials, the nano-encapsulated solution required ten times more product than when using the pure oils. Increasing the concentration of essential oil past 10% is not a viable solution as it would compromise the products stability, leading to faster degradation (Y. Feng, *personal communication*). Finally, phytotoxicity of the nano-encapsulated oil in the detached leaflet assay was less severe than the pure oils, but still present (Fig. 3.14). Although minimal, any level of phytotoxicity would be considered unacceptable in commercial production settings. Collectively, these limitations represent a significant barrier to the practicality of utilizing these products within commercial strawberry production systems (Thind 2021). Further product development is necessary to address the current limitations observed within this study and further research is required to investigate the environmental impacts and persistence of nano-encapsulated essential oils.

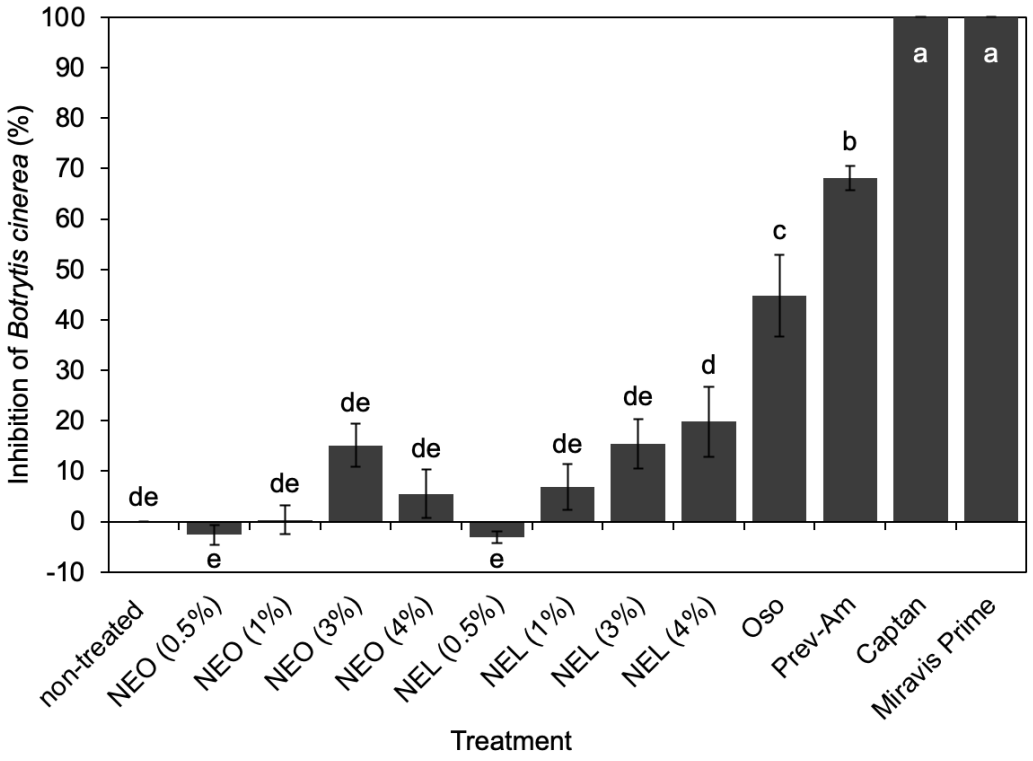

Figure 3.5. Average inhibition (%) of *Botrytis cinerea* according to the *in vitro* assay. NEO = nano-encapsulated orange oil; NEL = nano-encapsulated lemon oil. Values not connected by the same letter are significantly different ($P < 0.05$). Error bars represent the standard error of means (n = 4).

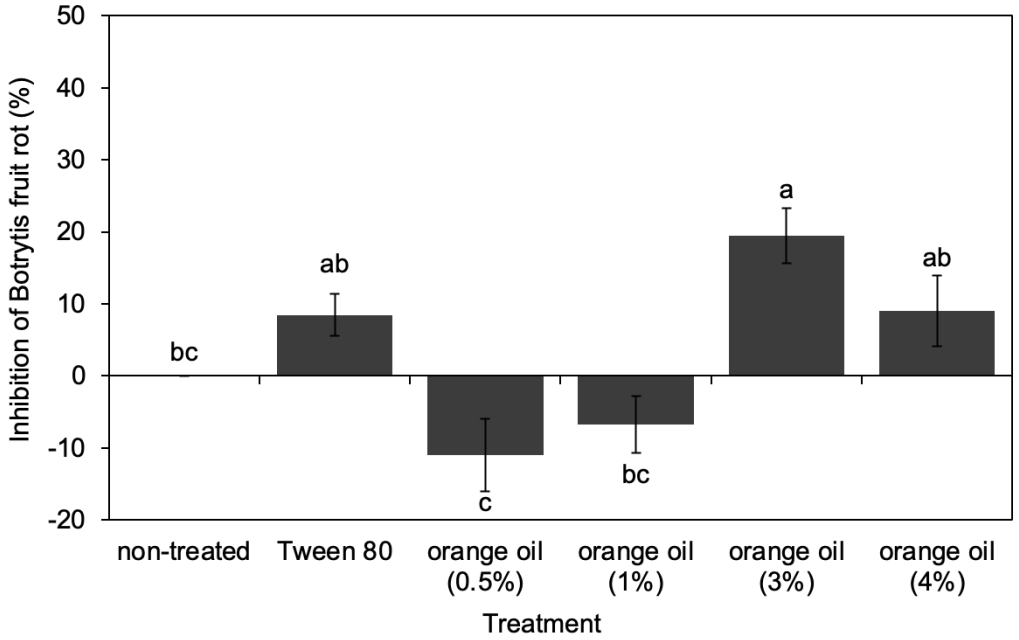

Figure 3.6. Average inhibition (%) of Botrytis fruit rot according to the detached fruit bioassay. Values not connected by the same letter are significantly different ($P < 0.05$). Error bars represent the standard error of means (n = 3).

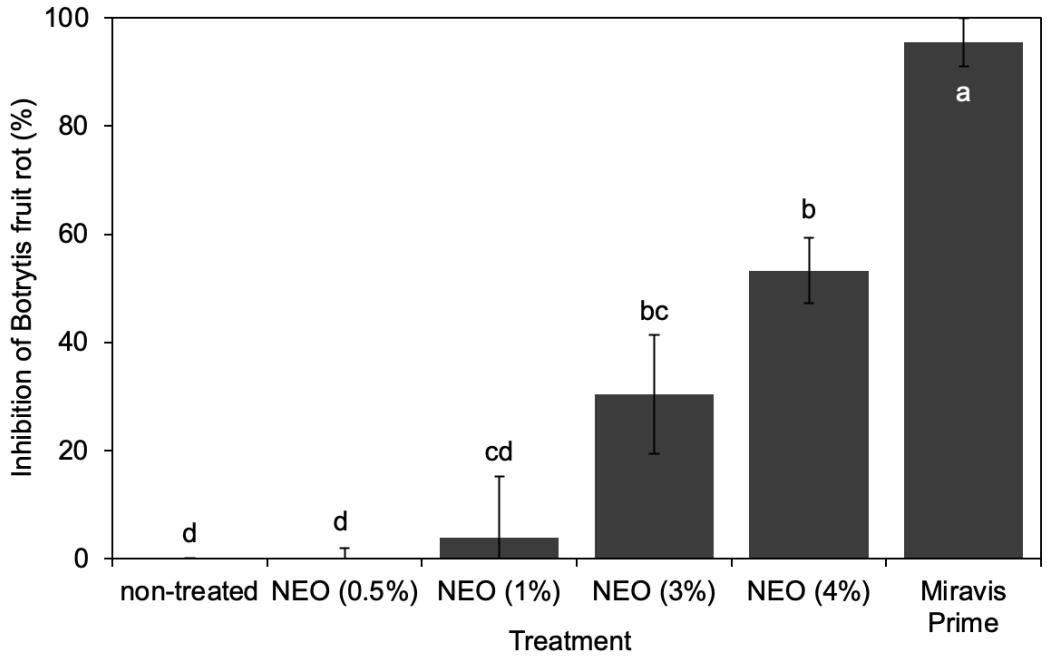

Figure 3.7. Average inhibition (%) of Botrytis fruit rot according to the detached fruit bioassay. NEO = nano-encapsulated orange oil. Values not connected by the same letter are significantly different ($P < 0.05$). Error bars represent the standard error of means (n = 3).

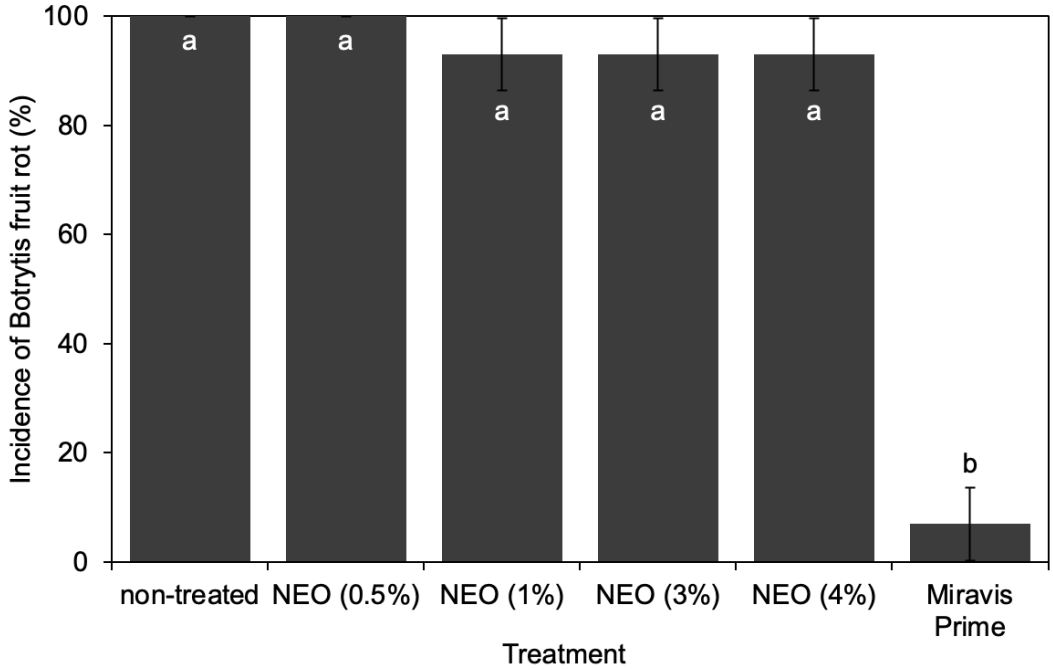

Figure 3.8. Average incidence (%) of Botrytis fruit rot according to the detached fruit bioassay. NEO = nano-encapsulated orange oil. Values not connected by the same letter are significantly different ($P < 0.05$). Error bars represent the standard error of means (n = 3).

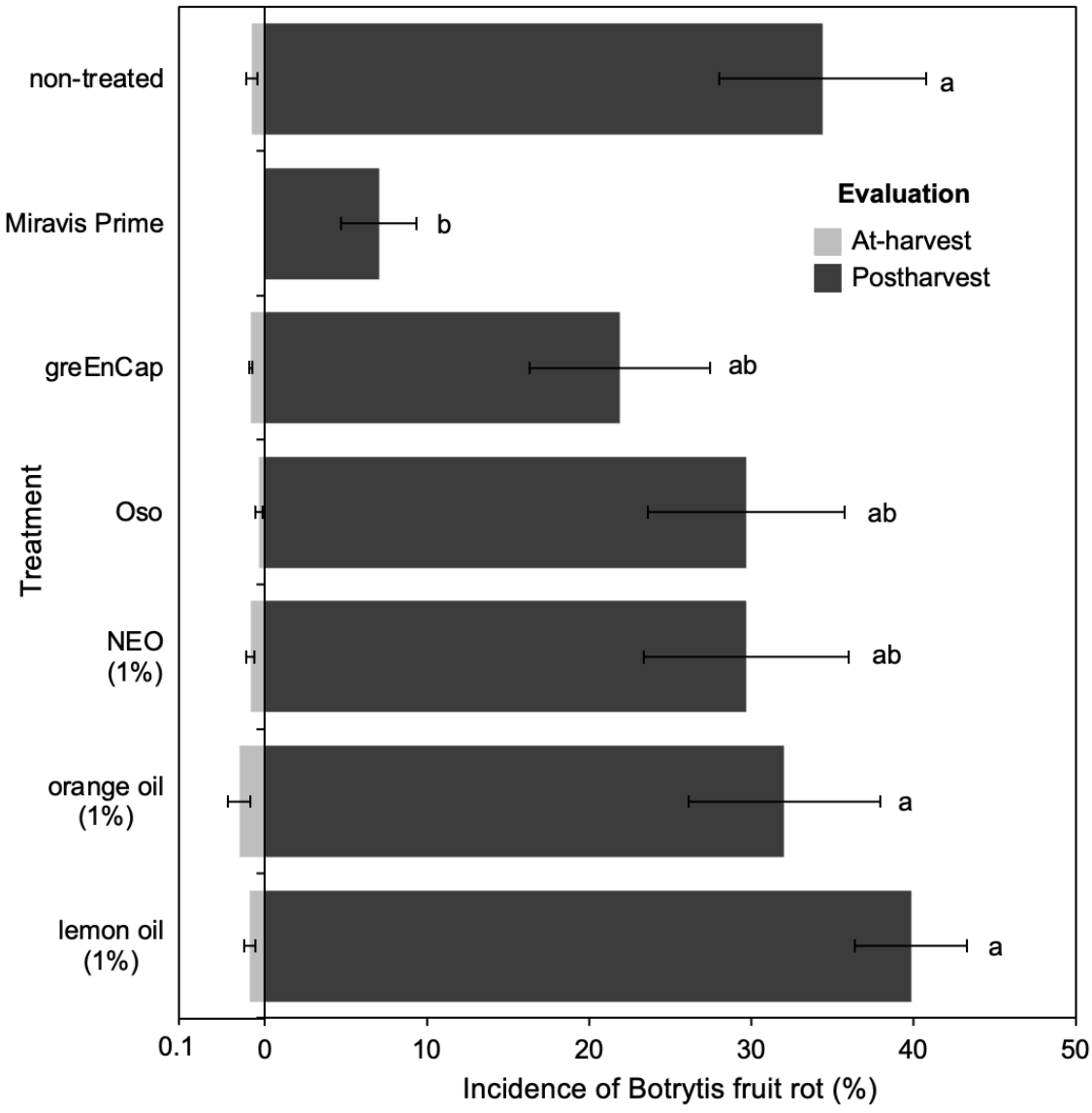

Figure 3.9. Average incidence (%) of Botrytis fruit rot within the field trial according to the at-harvest evaluation and the postharvest evaluation at four days after harvest. NEO = nano-encapsulated orange oil. Values not connected by the same letter are significantly different ($P < 0.05$). Error bars represent the standard error of means (n = 4).

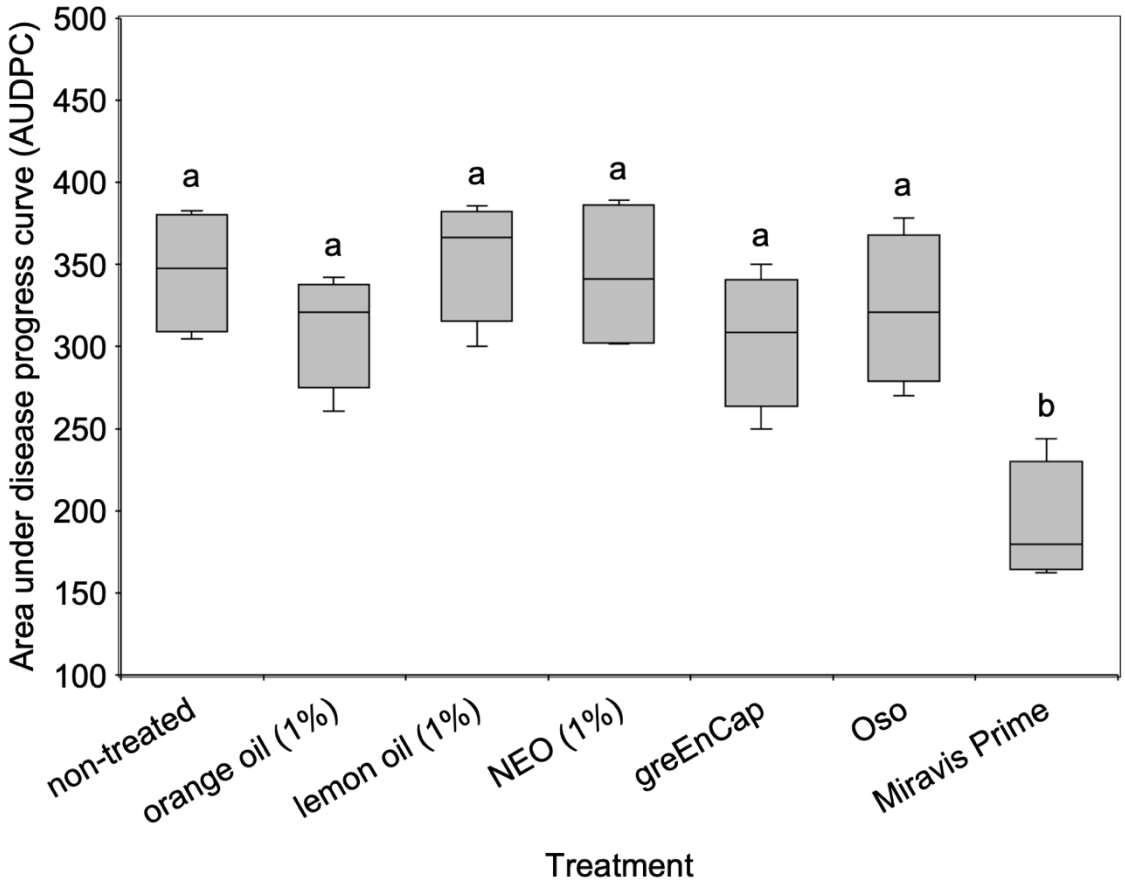

Figure 3.10. Area under the disease progress curve (AUDPC) of Botrytis fruit rot incidence in the field trial, according to the postharvest evaluation. NEO = nano-encapsulated orange oil. Values not connected by the same letter are significantly different ($P < 0.05$). Error bars represent the standard error of means (n = 4).

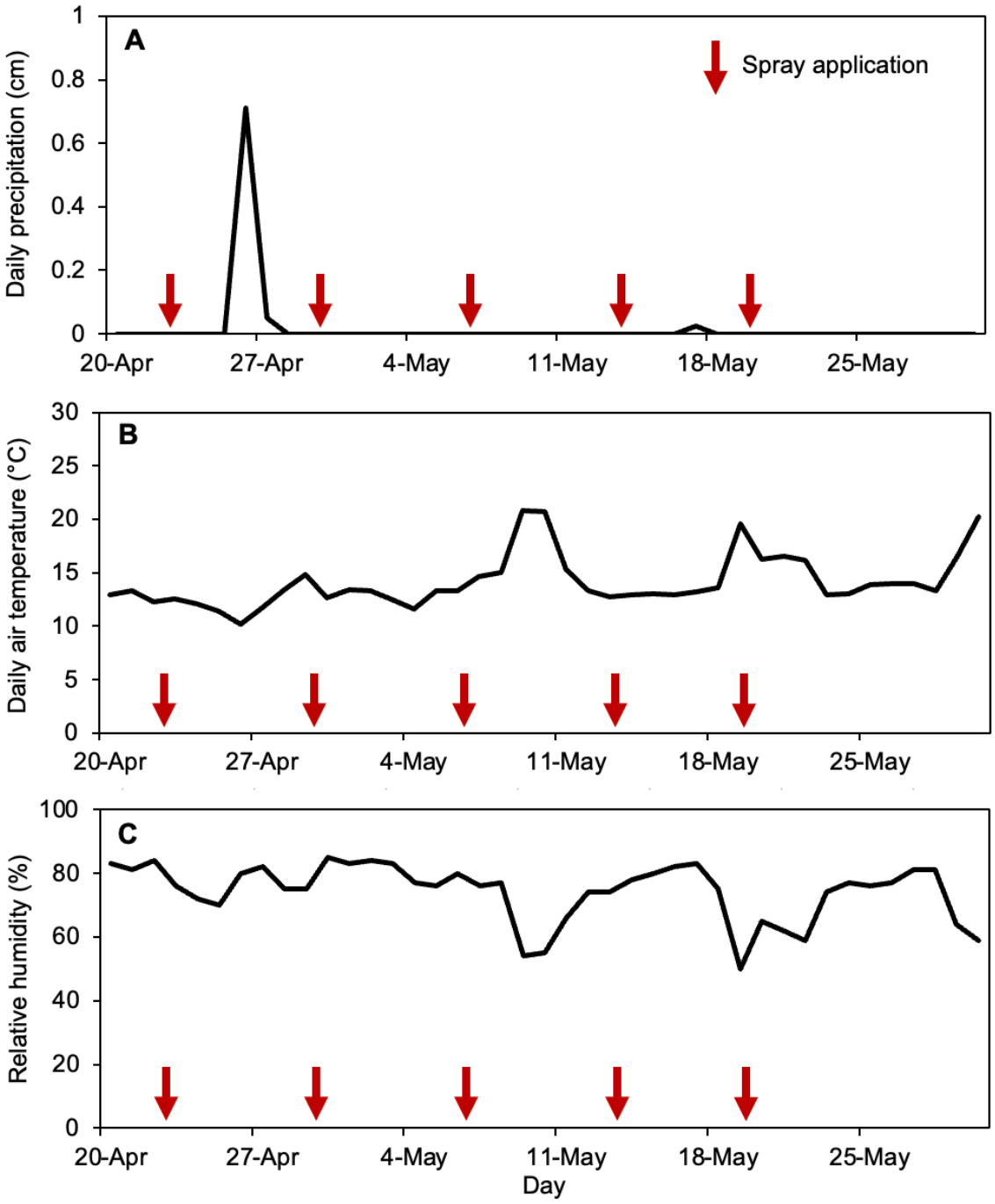

Figure 3.11. Daily (A) total precipitation (cm), (B) average air temperature (°C), and (C) average relative humidity (%) during the in-field experiment in 2025. Data were obtained from California Irrigation Management Information System (CIMIS) station #52.

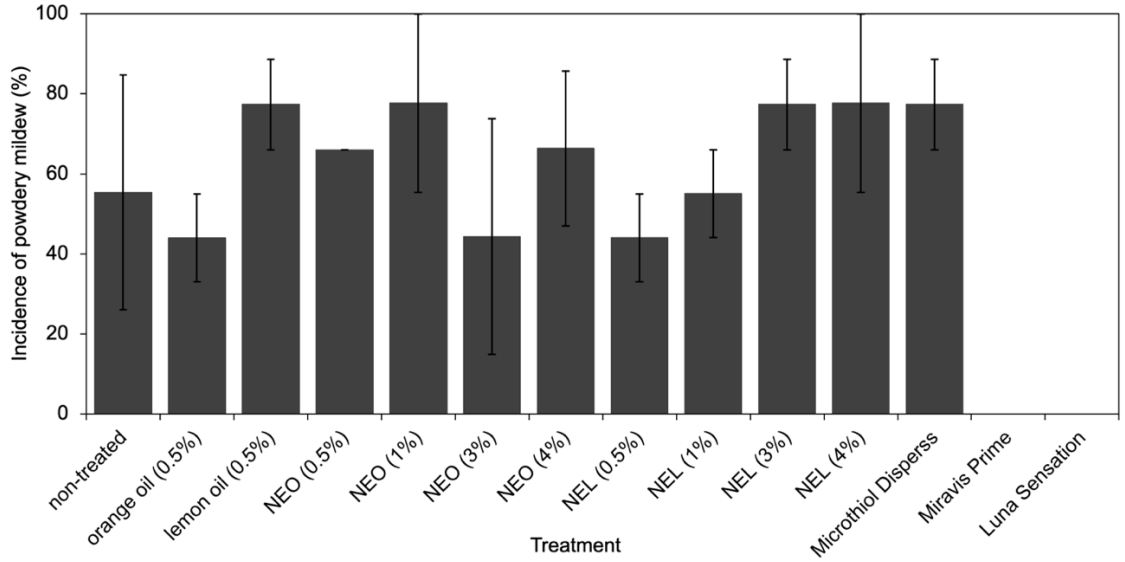

Figure 3.12. Average incidence (%) of *Podosphaera aphanis* according to the detached leaflet bioassay. NEO = nano-encapsulated orange oil; NEL = nano-encapsulated lemon oil. Values not connected by the same letter are significantly different ($P < 0.05$). Error bars represent the standard error of means (n = 3).

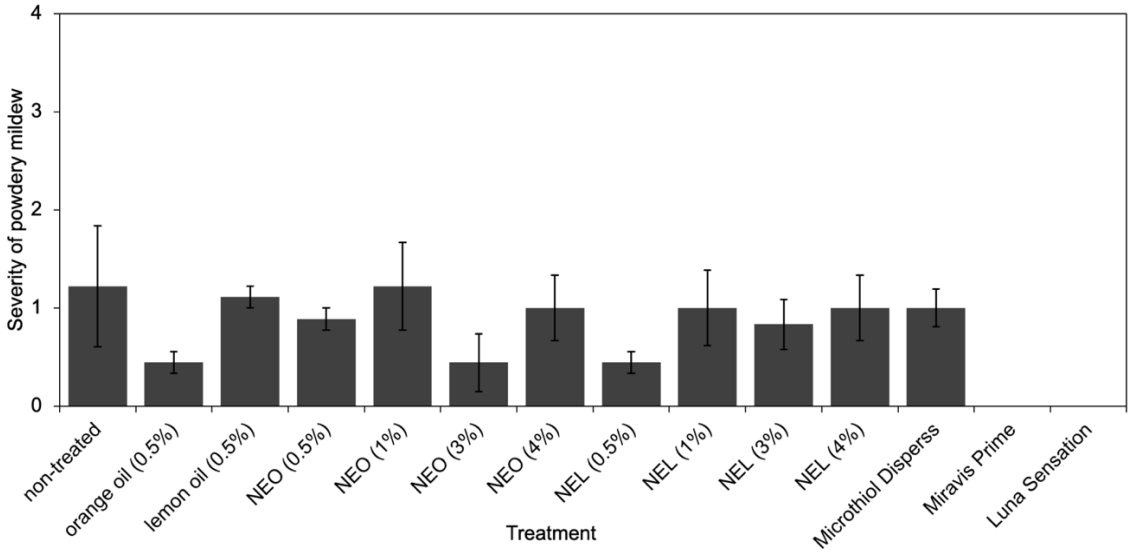

Figure 3.13. Average severity of *Podosphaera aphanis* according to the detached leaflet bioassay. NEO = nano-encapsulated orange oil; NEL = nano-encapsulated lemon oil. Values not connected by the same letter are significantly different ($P < 0.05$). Error bars represent the standard error of means (n = 3).

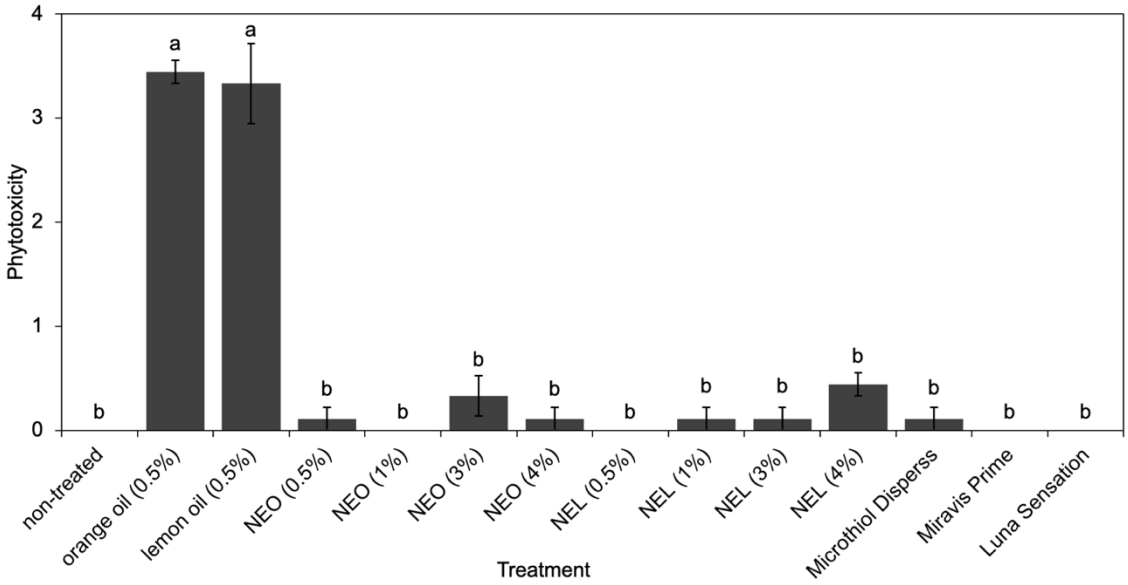

Figure 3.14. Average phytotoxicity observed within each treatment according to the detached leaflet bioassay. NEO = nano-encapsulated orange oil; NEL = nano-encapsulated lemon oil. Values not connected by the same letter are significantly different ($P < 0.05$). Error bars represent the standard error of means (n = 3).

REFERENCES

Adaskaveg, J. E., Michailides, T., and Eskalen, A. 2025. Fungicides, bactericides, biocontrols, and natural products for deciduous tree fruit and nut, citrus, strawberry, and vine crops in California. University of California Division of Agriculture and Natural Resources, Available at: https://ipm.ucanr.edu/legacy_assets/PDF/PMG/fungicideefficacytiming.pdf.

Ali, E. O. M., Shakil, N. A., Rana, V. S., Sarkar, D. J., Majumder, S., Kaushik, P., Singh, B. B., and Kumar, J. 2017. Antifungal activity of nano emulsions of neem and citronella oils against phytopathogenic fungi, *Rhizoctonia solani* and *Sclerotium rolfsii.* Ind. Crops Prod. 108:379-387.

Al-Shorafa, W., Mahadeen, A., and Al-Absi, K. 2014. Evaluation for salt stress tolerance in two strawberry cultivars. Am. J. Agric. Biol. Sci. 9:334-341.

Amsalem, L., Freeman, S., Rav-David, D., Nitzani, Y., Sztejnberg, A., Pertot, I., and Elad, Y. 2006. Effect of climatic factors on powdery mildew caused by *Sphaerotheca macularis* f. sp. *fragariae* on strawberry. Eur. J. Plant Pathol. 114:283-292.

Andersen, A. A. 1958. New sampler for the collection, sizing, and enumeration of viable airborne particles. J. Bacteriol. 76:471-484.

Arif, Y., Singh, P., Siddiqui, H., Bajguz, A., and Hayat, S. 2020. Salinity induced physiological and biochemical changes in plants: An omic approach towards salt stress tolerance. Plant Physiol. Biochem. 156:64-77.

Asalf, B., Transdem, N., Stensvand, A., Wekesa, V. W., de Moraes, G. J., and Klingen, I. 2012. Influence of sulfur, powdery mildew, and the predatory mite *Phytoseiulus persimilis* on two-spotted spider mite in strawberry. Biol. Control 61:121-127.

Asalf, B., Gadoury, D. M., Tronsmo, A. M., Seem, R. C., Cadle-Davidson, L., Brewer, M. T., and Stensvand, A. 2013. Temperature regulates the initiation of chasmothecia in powdery mildew of strawberry. Phytopathology 103:717-724.

Asalf, B., Gadoury, D. M., Tronsmo, A. M., Seem, R. C., and Stensvand, A. 2016. Effects of development of ontogenic resistance in strawberry leaves upon pre- and postgermination growth and sporulation of *Podosphaera aphanis*. Plant Dis. 100:72-78.

Asalf, B., Onofre, R. B., Gadoury, D. M., Peres, N. A., and Stensvand, A. 2020. Pulsed water mists for suppression of strawberry powdery mildew. Plant Dis. 105:71-77.

Avilés, M., Castillo, S., Borrero, C., Castillo, M. L., Zea-Bonilla, T., and Pérez-Jiménez, R. M. 2009. Response of strawberry cultivars: 'Camarosa', 'Candonga' and 'Ventana' to inoculation with isolates of *Macrophomina phaseolina*. Acta Hortic. 842:291-294.

Ayers, R. S., and Westcot, D. W. 1985. Management of salinity problems in: Water quality for agriculture. Food and Agriculture Organization Irrigation and Drainage Paper, Rome, IT.

Baggio, J. S., Cordova, L. G., Seijo, T. E., Noling, J. W., Whitaker, V. M., and Peres, N. A. 2021a. Cultivar selection is an effective and economic strategy for managing charcoal rot of strawberry in Florida. Plant Dis. 105:2033-2234.

Baggio, J. S., Ruschel, R. G., Noling, J. W., and Peres, N. A. 2021b. Physical, cultural, and chemical alternatives for integrated management of charcoal rot of strawberry. Plant Dis. 105:295-304.

Blauer, K. A., and Holmes, G. J. 2023. Effects of plastic mulch color and number of drip irrigation lines on incidence of Macrophomina root rot. Annual NASGA Meeting & North American Strawberry Symposium, San Luis Obispo, CA. Available at: https://content-calpoly-edu.s3.amazonaws.com/strawberry/1/documents/Effects%20of%20Plastic%20Mulch%20Color%20and%20Number%20of%20drip%20lines%2C%20NASGA%202023%20PDF%20friendly.pdf.

Blauer, K. A., and Holmes, G. J. 2019. Evaluation of pre-plant dip, biofumigant, and soil drench treatments to control Macrophomina crown rot on fall planted strawberries, 2019. Plant Dis. Manag. Rep. 14:PF050.

California Department of Food and Agriculture (CDFA). 2024. California agricultural production statistics. CDFA, Available at: https://www.cdfa.ca.gov/statistics/.

California Department of Pesticide Regulation (DPR). 2023. Pesticide use annual report: 2023 data summary. DPR, Available at: https://www.cdpr.ca.gov/pesticide-use-in-california/pesticide-use-reporting/pesticide-use-reporting-2023-summary-data/.

California Irrigation Management Information System (CIMIS). 2025. California Department of Water Resources.

California Soil Resource Lab, UC Davis/UC-ANR/USDA NRCS. 2024. SoilWeb. https://casoilresource.lawr.ucdavis.edu/gmap/.

California Strawberry Commission (CSC). 2024a. Economic Impact. CSC.

California Strawberry Commission (CSC). 2024b. The pink sheet. CSC, Available at: https://calstrawberry1.sharepoint.com/sites/IndustryPortal-Landing/SitePages/MD-Pink-Sheet.aspx.

Callaway, T. R., Carroll, J. A., Arthington, J. D., Edrington, T. S., Anderson, R. C., Ricke, S. C., Crandall, P., Collier, C., and Nisbet, D. J. 2011. Citrus products and their use against bacteria: Potential health and cost benefits. Pages 227-286 in: Nutrients, dietary supplements, and nutriceuticals: Cost analysis versus clinical benefits. R. R. Watson, J. K. Gerald and V. R. Preedy, eds. Humana Press, New York, NY.

Chilakala, A. R., Mali, K. V., Irulappan, V., Patil, B. S., Pandey, P., Rangappa, K., Ramegowda, V., Kumar, M. N., Puli, C. O. R., Mohan-Raju, B., and Senthil-Kumar, M. 2022. Combined drought and heat stress influences the root water relation and determine the dry root rot disease development under field conditions: A study using contrasting chickpea genotypes. Front. Plant Sci. 13:890551.

Cloud, G. L., and Rupe, J. C. 1991. Comparison of three media for enumeration of sclerotia of *Macrophomina phaseolina*. Plant Dis. 75:771-772.

Cosseboom, S. D., Ivors, K. I., Schnabel, G., Bryson, P. K., and Holmes, G. J. 2019. Within-season shift in fungicide resistance profiles of *Botrytis cinerea* in California strawberry fields. Plant Dis. 103:59-64.

Cordova, L. G., A., A., and Peres, N. A. 2017. Effectiveness of fungicide treatments following the Strawberry Advisory System for control of Botrytis fruit rot in Florida. Crop Prot. 100:163-167.

Dahikar, S., and Nagarkar, R. 2023. Development of tolerance by *Macrophomina phaseolina* against fungicide, insecticide, and drought. Pages 225-237 in: *Macrophomina phaseolina*: Ecobiology, Pathology and Management. P. Kumar and R. C. Dubey, eds. Academic Press, London, U. K.

Darrow, G. M. 1966. The strawberry: History, breeding, and physiology. Holt, Rinehart & Winston, New York, NY.

Davis, T. M., Denoyes-Rothan, B., and Lerceteau-Köhler, E. 2007. Strawberry. Pages 189-205 in: Fruits and nuts: Genome mapping and molecular breeding in plants, vol. 4. C. Kole, ed. Springer, Berlin, Heidelberg.

Dhingra, O. D., and Sinclair, J. B. 1974. Survival of *Macrophomina phaseolina* sclerotia in soil: Effects of soil moisture, carbon:nitrogen ratios, carbon sources, and nitrogen concentrations. Phytopathology 65:236-240.

Donsì, F., and Ferrari, G. 2016. Essential oil nanoemulsions as antimicrobial agents in food. J. Biotechnol. 233:106-120.

Duniway, J. M. 2002. Status of chemical alternatives to methyl bromide for pre-plant fumigation of soil. Phytopathology 92:1337-1343.

Dwivedi, M., Rai, R. K., and Singh, P. 2025. Evaluating innovative strategies for managing strawberry fruit rot diseases: Insight from current research. Stud. In Fungi 10:e012.

El Asbahani, A., Miladi, K., Badri, W., Sala, M., Aït Addi, E. H., Casabianca, H., El Mousadik, A., Hartmann, D., Jilale, A., Renaud, F. N. R., and Elaissari, A. 2015. Essential oils: From extraction to encapsulation. Int. J. Pharm. 483:220-243.

Ellis, M. B., and Waller, J. M. 1974. *Sclerotinia fuckeliana* (conidial state: *Botrytis cinerea*). CMI Descriptions of Pathogenic Fungi and Bacteria. No. 431. Commonwealth Mycological Institute, Kew, England.

Erwin, D. C. and Ribeiro, O. K. 1996. Phytophthora diseases worldwide. American Phytopathological Society Press. St. Paul, MN.

Food and Agriculture Organization of the United Nations (FAO). 2023. Top 10 country production of strawberries. FAO.

Fungicide Resistance Action Committee (FRAC). 2019. Pathogen risk list. FRAC, Available at: https://www.frac.info/media/oqljqgdi/frac-pathogen-list-2019.pdf.

Gago, C. M. L., Artiga-Artigas, M., Antunes, M. D. C., Faleiro, M. L., Miguel, M. G., and Martín-Belloso, O. 2019. Effectiveness of nanoemulsions of clove and lemongrass essential oils and their major components against *Escheritchia coli* and *Botrytis cinerea* J. Food Sci. Technol. 56:2721-2736.

Goudarzi, A., Banihashemi, Z., and Maftoun, M. 2011. Effect of salt and water stress on root infection by *Macrophomina phaseolina* and ion composition in shoot in sorghum. Iran. J. Plant Pathol. 47:69-83.

Gupta, A., Jeyakumar, E., and Lawrence, R. 2021. Journey of limonene as an antimicrobial agent. J. Pure Appl. Microbiol. 15:1094-1110.

Hahn, M. 2014. The rising threat of fungicide resistance in plant pathogenic fungi: *Botrytis* as a case study. J. Chem. Biol. 7:133-141.

Hobbelen, P. H. F., Paveley, N. D., and van den Bosch, F. 2014. The emergence of resistance to fungicides. PLoS ONE 9:e91910.

Holmes, G. J., Mansouripour, S. M., and Hewavitharana, S. S. 2020. Strawberries at the crossroads: Management of soilborne diseases in California without methyl bromide. Phytopathology 110:956-1117.

Holmes, G. J. 2024. The California strawberry industry: Current trends and future prospects. Int. J. Fruit Sci. 24:115-129.

Ivushkin, K., Bartholomeus, H., Bregt, A. K., Pulatov, A., Franceschini, M. H. D., Kramer, H., van Loo, E. N., Roman, V. J., and Finkers, R. 2019. UAV based soil salinity assessment of cropland. Geoderma 338:502-512.

Janisiewicz, W. J., Takeda, F., Nichols, B., Glenn, D. M., Jurick II, W. M., and Camp, M. J. 2016. Use of low-dose UV-C irradiation to control powdery mildew caused by *Podosphaera aphanis* on strawberry plants. Can. J. Plant Pathol. 38:430-439.

Jarvis, W. R. 1962. The infection of strawberry and raspberry fruits by *Botrytis cinerea* Fr. Ann. Appl. Biol. 50:569-575.

Jeger, M. J., and Vilijanen-Rollinson, S. L. H. 2001. The use of the area under the disease-progress curve (AUDPC) to assess quantitative disease resistance in crop cultivars. Theor. Appl. Genet. 102:32-40.

Kabir, Z., Bhat, R. G., and Subbarao, K. V. 2004. Comparison of media for recovery of *Verticillium dahliae* from soil. Plant Dis. 88:49-55.

Kale, P. N., and Adsule, P. G. 1995. Citrus. Pages 39-65 in: Handbook of Fruit Science and Technology: Production, Composition, Storage, and Processing. D. K. Salunkhe and S. S. Kadam, eds. Marcel Dekker Inc., New York, NY.

Kaur, S., Dhillon, G. S., Brar, S. K., Vallad, G. E., Chand, R., and Chauhan, V. B. 2012. Emerging phytopathogen *Macrophomina phaseolina*: Biology, economic importance and current diagnostic trends. Crit. Rev. Microbiol. 38:136-151.

Kendig, S. R., Rupe, J. C., and Scott, H. D. 2000. Effect of irrigation and soil water stress on densities of *Macrophomina phaseolina* in soil and roots of two soybean cultivars. Plant Dis. 84:895-900.

Khalili, E., Kamyab, H., Balasubramanian, B., and Chelliapan, S. 2026. Integrated management of charcoal rot (*Macrophomina phaseolina*) in soybean: Current strategies and the emerging role of β-glucosidase. Appl. Soil Ecol. 217:106549.

Khetabi, A. E., Lahlali, R., Ezrari, S., Radouane, N., Lyousfi, N., Banani, H., Askarne, L., Tahiri, A., Ghadraoui, L. E., Belmalha, S., and Barka, E. A. 2022. Role of plant extracts and essential oils in fighting against postharvest fruit pathogens and extending fruit shelf life: A review. Trends Food Sci. Technol. 120:402-417.

Klamkowski, K., and Treder, W. 2006. Morphological and physiological responses of strawberry plants to water stress. Agric. Conspec. Sci. 71:159-165.

Knapp, S. J., Cole, G. S., Pincot, D. D. A., Dilla-Ermita, C. J., Bjornson, M., Famula, R. A., Gordon, T. R., Harshman, J. M., Henry, P. M., and Feldmann, M. J. 2024. Transgressive segregation, hopeful monsters, and phenotypic selection drove rapid genetic gains and breakthroughs in predictive breeding for quantitative resistance to *Macrophomina* in strawberry. Hortic. Res. 11:1-22.

Koike, S. T. 2008. Crown rot of strawberry caused by *Macrophomina phaseolina* in California. Plant Dis. 92:1253.

Koike, S. T., Gordon, T. R., Daugovish, O., Ajwa, H., Bolda, M., and Subbarao, K. 2013. Recent developments on strawberry plant collapse problems in California caused by *Fusarium* and *Macrophomina*. Int. J. Fruit Sci. 13:76-83.

Koike, S. T., Arias, R. S., Hogan, C. S., Martin, F. N., and Gordon, T. R. 2016. Status of *Macrophomina phaseolina* on strawberry in California and preliminary characterization of the pathogen. Int. J. Fruit Sci. 16:148-159.

Ledesma, F., Lopez, C., Ortiz, D., Chen, P., Korth, K. L., Ishibashi, T., Zeng, A., Orazaly, M., and Florez-Palacios, L. 2016. A simple greenhouse method for screening salt tolerance in soybean. Crop Sci. 56:1-10.

Legard, D. E., Xiao, C. L., Mertely, J. C., and Chandler, C. K. 2000. Effects of plant spacing and cultivar on incidence of Botrytis fruit rot in annual strawberry. Plant Dis. 84:531-538.

Lin, H., Li, Z., Sun, Y., Zhang, Y., Wang, S., Zhang, Q., Ting, C., Xiang, W., Zeng, C., and Tang, J. 2024. *D*-limonene: Promising and sustainable natural bioactive compound. Appl. Sci. 14:4605.

Maas, E. V., and Hoffman, G. J. 1977. Crop salt tolerance—Current assessment. J. Irrig. Drain. Div. 103:115-134.

Menzel, C. M. 2021. A review of powdery mildew in strawberries: The resistance of species, hybrids and cultivars to the pathogen is highly variable within and across studies with no standard method for assessing the disease. J. Hortic. Sci. Biotechnol. 97:273-297.

Mertely, J. C., Chandler, C. K., Xiao, C. L., and Legard, D. E. 2000. Comparison of sanitation and fungicides for management of Botrytis fruit rot of strawberry. Plant Dis. 84:1197-1202.

Mertely, J. C., MacKenzie, S. J., and Legard, D. E. 2002. Timing of fungicide applications for *Botrytis cinerea* based on development stage of strawberry flowers and fruit. Plant Dis. 86:1019-1024.

Miastkowska, M., Michalczyk, A., Figacz, K., and Sikora, E. 2020. Nanoformulations as a modern form of biofungicide. J. Environ. Health. Sci. Eng. 18:119-128.

Mihail, J. D. 1992. *Macrophomina*. Pages 134-136 in: Methods for research on soilborne phytopathogenic fungi. L. L. Singleton, J. D. Mihail, and C. M. Rush, eds. American Phytopathological Society Press, St. Paul, MN.

Morishita, M., Sugiyama, K., Saito, T., and Sakata, Y. 2003. Powdery mildew resistance in cucumber. Jpn. Agric. Res. Q. 37:7-14.

Onofre, R. B., Gadoury, D. M., Stensvand, A., Bierman, A., Rea, M., and Peres, N. A. 2021a. Use of ultraviolet light to suppress powdery mildew in strawberry fruit production fields. Plant Dis. 105:2402-2409.

Onofre, R. B., Gadoury, D. M., and Peres, N. A. 2021b. High efficacy and low risk of phytotoxicity of sulfur in the suppression of strawberry powdery mildew. Plant Health Prog. 22:101-107.

Palmer, M. G., and Holmes, G. J. 2021. Fungicide sensitivity in strawberry powdery mildew caused by *Podosphaera aphanis* in California. Plant Dis. 105:2601-2605.

Palmer, M. G., and Holmes, G. J. 2022. Characterization of strawberry host plant resistance to powdery mildew caused by *Podosphaera aphanis*. Plant Health Prog. 23:82-86.

Pedroncelli, L., Biscaro, A., and Putman, A. I. 2025. Role of soil moisture in disease development of charcoal rot of strawberries caused by *Macrophomina phaseolina*. Plant Dis. 109:1268-1279.

Pennerman, K. K., Dilla-Ermita, C. J., and Henry, P. M. 2024. Exaggerated plurivory of *Macrophomina phaseolina*: Accounting for the large host range claim and the shifting of scientific language. Phytopathology 114:119-125.

Ramirez, J. A. 2024. Improved management strategies for Botrytis fruit rot, Macrophomina root rot, and Verticillium wilt in California strawberry production [thesis]. California Polytechnic State University, San Luis Obispo.

Rhoades, J. D. 1974. Drainage for salinity control. Pages 433-462 in: Drainage for agriculture. J. Van Schilfgaarde, ed. American Society of Agronomy, Inc., Madison, WI.

Romanazzi, G., and Feliziani, E. 2014. *Botrytis cinerea* (Gray mold). Pages 131-146 in: Postharvest decay: Control strategies. S. Bautista-Baños, ed. Academic Press, London, UK.

Romanazzi, G., Feliziani, E., and Peres, N. A. 2022. Postharvest diseases of strawberry. Pages 295-314 in: Postharvest pathogology of fruit and nut crops: Principles, concepts, and management practices. J. E. Adaskaveg, H. Förster and D. B. Prusky, eds. The American Phytopathological Society, St. Paul, MN.

Santos-Gomes, P. C., and Fernandes-Ferreira, M. 2001. Organ- and season-dependent variation in the essential oil composition of *Salvia officinalis* L. cultivated at two different sites. J. Agric. Food. Chem. 49:2908-2916.

Sarr, M. P., Ndiaye, M., and Cisse, N. 2023. Morphological and physiological characterization of *Macrophomina* isolates from Senegal. Pages 9-19 in: *Macrophomina phaseolina*: Ecobiology, Pathology and Management. P. Kumar and R. C. Dubey, eds. Academic Press, London, U. K.

Seleiman, M. F., Al-Suhaibani, N., Ali, N., Akmal, M., Alotaibi, M., Refay, Y., Dindaroglu, T., Abdul-Wajid, H. H., and Battaglia, M. L. 2021. Drought stress impacts on plants and different approaches to alleviate its adverse effects. Plants 10:259.

Sharath Chandran, U. S., Tarafdar, A., Mahesha, H. S., and Sharma, M. 2021. Temperature and soil moisture stress modulate the host defense response in chickpea during dry root rot incidence. Front. Plant Sci. 12:653265.

Shehata, S. A., Abdeldaym, E. A., Ali, M. R., Mohamed, R. M., Bob, R. I., and Abdelgawad, K. F. 2020. Effect of some citrus essential oils on post-harvest shelf life and physicochemical quality of strawberries during cold storage. Agronomy 10:1466.

Simard, S. Z. 2024. Survey of soilborne pathogens infecting strawberry in Oxnard, California & effect of planting date and chill treatment on the yield of strawberry [thesis]. California Polytechnic State University, San Luis Obispo.

Singh, S., Prashad, H., and Gautam, H. 2023. Management of *Macrophomina phaseolina* by cultural practices. Pages 225-237 in: *Macrophomina phaseolina*: Ecobiology, Pathology, and Management, P. Kumar and R. C. Dubey, eds. Academic Press, London, U.K.

Soleimani, H., Mostowfizadeh-Ghalamfarsa, R., Ghanadian, M., Karami, A., and Cacciola, S. O. 2023. Defense mechanisms induced by celery seed essential oil against powdery mildew incited by *Podosphaera fusca* in cucumber. J. Fungi 10:17.

Soleimani, H., Mostowfizadeh-Ghalamfarsa, R., and Zarei, A. 2024. Chitosan nanoparticle encapsulation of celery seed essential oil: Antifungal activity and defense mechanisms against cucumber powdery mildew. Carbohydr. Polym. Technol. Appl. 8:100531.

Steele, M. E. 2023. Soilborne pathogens of strawberry in California's central coast: Survey and wheat cover cropping for management of *Macrophomina phaseolina* [thesis]. California Polytechnic State University, San Luis Obispo.

Steele, M. E., Hewavitharana, S. S., Henry, P. M., Goldman, P., and Holmes, G. J. 2023. Survey of late-season soilborne pathogens infecting strawberry in Watsonville-Salinas, California. Plant Health Prog. 24:104-109.

Steele, M. E., Mendez, M., Hewavitharana, S. S., and Holmes, G. J. 2024. Survey of soilborne pathogens infecting strawberry in Santa Maria, California. Int. J. Fruit Sci. 23:256-266.

Strand, L. L. 2008. Integrated pest management for strawberries, Second Ed. Publi. No. 3351. University of California Press, Oakland, CA.

Teja, T. S., Kelayia, D. S., and Asha, R. 2020. Impact of environmental factors on *Macrophomina phaseolina* causing charcoal rot of soybean. Int. J. Curr. Microbiol. Appl. Sci. 9:3784-3790.

Thind, T. S. 2021. Changing trends in discovery of new fungicides: A perspective. Indian Phytopathol. 74:875-883.

Turek, C., and Stintzing, F. C. 2013. Stability of essential oils: A review. Compr. Rev. Food Sci. Food Saf. 12:40-53.

Turhan, E., and Eriș, A. 2007. Growth and stomatal behavior of two strawberry cultivars under long-term salinity stress. Turk. J. Agric. For. 31:55-61.

University of California Integrated Pest Management (UC IPM). 2018. Powdery mildew: *Podosphaera aphanis*. UC IPM, Available at: https://ipm.ucanr.edu/agriculture/strawberry/powdery-mildew.

University of California Integrated Pest Management (UC IPM). 2025. Managing pesticide resistance. UC IPM, Available at: https://ipm.ucanr.edu/agriculture/floriculture-and-ornamental-nurseries/managing-pesticide-resistance/#gsc.tab=0.

Vilas-Franquesa, A., Saldo, J., and Juan, B. 2022. Sea buckthorn (*Hippophae rhamnoides*) oil extracted with hexane, ethanol, diethyl ether and 2-MTHF at different temperatures - An individual assessment. J. Food Compos. Anal. 114:104752.

Wang, Y. C., Mansouripour, S. M., Hewavitharana, S. S., and Holmes, G. J. 2024. Effect of cultivar and temperature on disease development of Macrophomina root rot in strawberry. Plant Health Prog. 25:255-261.

Werrie, P. Y., Durenne, B., Delaplace, P., and Fauconnier, M. L. 2020. Phytotoxicity of essential oils: Opportunities and constraints for the development of biopesticides. A review. Foods 9:1291.

Williamson, B., Tudzynski, B., Tudzynski, P., and van Kan, J. A. L. 2007. *Botrytis cinerea*: The cause of grey mould disease. Mol. Plant Pathol. 8:561-580.

Xiao, C. L., Chandler, C. K., Price, J. F., Duval, J. R., Mertely, J. C., and Legard, D. E. 2001. Comparison of epidemics of Botrytis fruit rot and powdery mildew of strawberry in large plastic tunnel and field production systems. Plant Dis. 85:901-909.

You, M. P., Colmer, T. D., and Barbetti, M. J. 2011. Salinity drives host reaction in *Phaseolus vulgaris* (common bean) to *Macrophomina phaseolina*. Funct. Plant Biol. 38:984-992.

Zhang, H., Zhu, J., Gong, Z., and Zhu, J. K. 2022. Abiotic stress responses in plants. Nat. Rev. Genet. 23:104-119.

Zveibil, A., Mor, N., Gnayem, N., and Freeman, S. 2012. Survival, host-pathogen interaction, and management of *Macrophomina phaseolina* on strawberry in Israel. Plant Dis. 96:265-272.

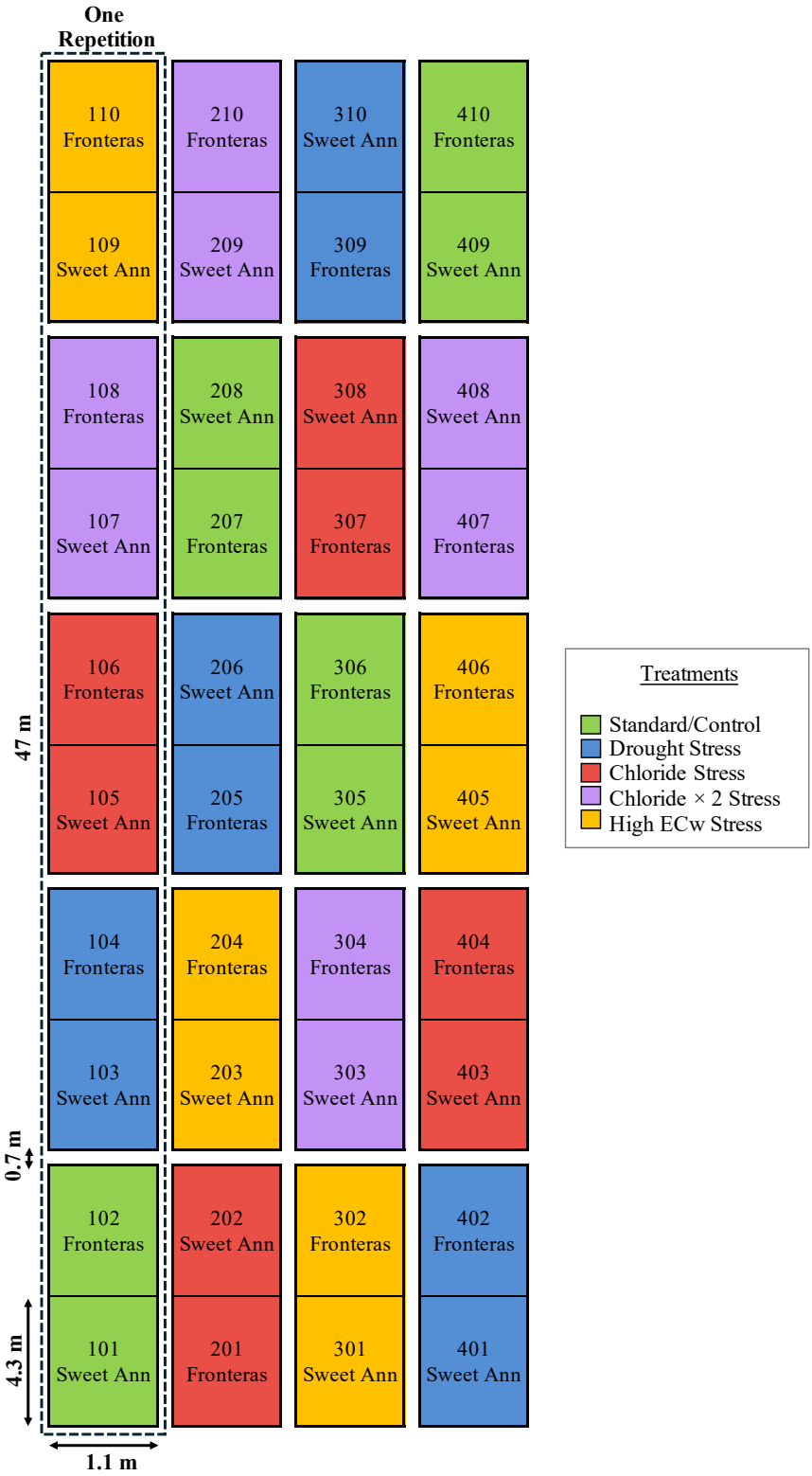

Figure 4.1. Split plot experimental design from the 2024 season showing cultivar (Fronteras or Sweet Ann), treatment type, and bed dimensions.